The morphodynamic influence of cohesive sediment on coastal systems across scales

A DISSERTATION
SUBMITTED TO THE FACULTY OF
UNIVERSITY OF MINNESOTA
BY

Antoinette Victoria Abeyta

IN PARTIAL FULFILLMENT OF THE REQUIREMENTS
FOR THE DEGREE OF
DOCTOR OF PHILOSOPHY

Dr. Chris Paola, Advisor

July 2016

Recipe for a Thesis

Contained within this dissertation is roughly:

- 216,048 liters of water
- 5,341 kg of kaolinite clay
- 9,115 kg of walnut shell sand
- 8,513 kg of quartz sand
- 488 hours of experimental run time
- 371,382 photographs
- 89 hours and 53 minutes of video
- 60 topographic scans
- 13 sonar scans
- 197 landslides
- 423 Matlab scripts
- 240 spreadsheets
- 89 references cited
- 32 figures
- 7 tables

To add up to a total of 3169 gigs of data contained within 86 pages.

Acknowledgements

Looking back at my time here as a graduate student, I am tremendously grateful for all the help and support I have received. My story starts back in 2007, when I first came to SAFL as an intern in Kimberly Hill's complex materials REU program. Without all the help and support of Pat Jones Whyte, Kimberly Hill, Diana Dalbotten and Karen Campbell, I would have never have gone to graduate school or pursued my doctorate. I owe a lot of my success to them for showing me that getting a doctorate is possible!

I have also been very fortunate to have Chris Paola as an advisor. Chris has an inherently strong curiosity of the world and drive to understand the world around him. I have learned so much from listening to him work through problems and his willingness to take risks. Thank you Chris for all your patience throughout all these years.

I am very thankful for Karen Gran, John Swenson and Brady Foreman for all their advice and guidance. I have learned through them how to become a better teacher, a better scholar and a better person.

The Community of Scholars Program has been like a second family to me, a caring group of individuals who always root for you when things get tough. I am very grateful for all the support, opportunities and sense of community that Noro Andriamanalina has created with COSP. I am also grateful for all the help and support from Jasmine Tang who worked with me to help me become a better writer.

I am very grateful to have spent my time at St. Anthony Falls Laboratory. SAFL is a rare community of people who work collaboratively and believe they can make anything work with enough duct tape, clamps and plumbers putty. Much of the research that I have done at SAFL would not have been possible without the help and support of Ben Erikson, Aaron Ketchmark, Erik Steen, Dick Christopher, Jim Mullen, Chris Ellis, Sarah Milke, Charles Nguyen, Danny Im, the SAFL tech staff and the SAFL IT staff. Sorry about the rotten walnut smell! I would also like to thank Barbara Burkholder-Heitkamp, Deb Pierzina, and all the other folks of the National Center for Earth Surface Dynamics for all the support and opportunities. I would also like to thank Sarah Baumgardner for all the help babysitting deltas.

I would also like to thank my committee Kimberly Hill, Emi Ito and Brandon Dugan. I am grateful for all their support, comments and time! Much thanks is also owed to Bonnie-Jean Mackay, Jenny Snyder, Sharon Kressler and Jen Petrie who make everything in the departments work.

Lastly, none of this would have been possible without the endless support of my family and friends. Thank you Mom, Dad, and Andrew for always being there for me and always believing in me. Also thanks to Goose and Spock for being cute and fuzzy.

For Mom, Dad, Andrew, Goose and Spock

Abstract

Cohesive sediment makes up a large portion of the rock record and much of the earth's surface sediment. Despite how common cohesive sediments are, the focus of research on sedimentary systems has largely been on non-cohesive sediment. Consequently, there has been limited research on how cohesive sediment influences sediment transport and the implications this has for depositional systems. To increase our knowledge of cohesive sediment, it is important to understand the morphological impact of cohesive sediment on depositional systems. Physical experiments provide a powerful tool for approaching this problem as they will allow us to constrain and measure parameters which may be difficult to measure in the field.

The overarching goal of this project is to expand our experimental framework to include the use of cohesive sediment, which allows us to investigate an important set of effects in the field. Presented here is a framework of physical experiments, which investigate quantitative aspects of how cohesive sediment influences morphodynamics across scales. The first experimental series investigates how mass failures form in cohesive sediment on delta fronts and what factors influence their occurrence and evolution. The second experimental series is a study on how cohesion influences deltaic processes and overall morphology. Finally, the last experimental series is on how cohesive and other fine sediment lead to changes in the gradient of sediment flux that in turn lead to upstream changes in the overall sediment mass balance in coastal systems.

CONTENTS

LIST OF TABLES

LIST OF FIGURES

INTRODUCTION

Depositional systems are composed of billions and billions of individual grains. Each of these grains set in motion by the forces of nature, with the tempo and deliberation of earth's processes. All of these particles are just "bits and pieces put together to present a semblance of a whole" (Weiner, 1991). Together, these grains weave a complex set of patterns and layers, creating a sort of 'epic poem of the earth' (Carson, 1951). As geologists, we long to understand how to translate this poem by reading the story of sediments. There has been extensive research to understand the movement of sediment, how it shapes our planet and more importantly, what these deposits tell us about the past.

The primary focus of our efforts to understand the language of sediment has largely centered on non-cohesive sediment. While this has led to many profound understandings of the language of sediment, many of these studies lack an important geomorphic threshold – cohesion. The role of cohesive sediment transport is often overlooked, despite the fact that clays and muds make over two thirds of the rock record and cover most of the earth's surface (Schieber et al, 1998). It is essential that we learn the language of shales and better understand the movement of cohesive sediment, such that we can translate the epic poem of the earth.

This dissertation is focused on the role of cohesive sediment in depositional systems across scales using physical laboratory experiments. Physical experiments allow for the study of sediment transport over space and time scales that are often inaccessible in the field. The chapters presented here, (1) Transport dynamics of mass failures along weakly cohesive clinoform foresets, (2) The morphodynamic influence of cohesive sediment in experimental deltas, and (3) Sink to source: the effect of offshore dynamics on upstream processes present findings that illustrate how the presence of cohesive sediment has changed the behavior of a depositional system across scales. As we look at these three different systems, we see how changes in the grain scale lead to measurable changes in the overall behavior. Understanding how these changes are manifested helps our understanding of the language of cohesive sediment.

REFERENCES

Carson, R. (1951) The long snowfall. Oxford Publishing: pp. 75-83.

Schieber, J. and **Zimmerle, W.**, 1998, The history and promise of shale research. *Shales and mudstones, 1, Basin studies of sedimentology and paleontology*, p. 1-10

Weiner, L., 1991, Walker Art Center.

1

TRANSPORT DYNAMICS OF MASS FAILURES ALONG WEAKLY COHESIVE CLINOFORM FORESETS*

*Published as Abeyta, A. and Paola, C. (2014) Transport dynamics of mass failures along weakly cohesive clinoform foresets. *Sedimentology*, 62, p. 303-313.

SUMMARY

This study addresses the initiation mechanisms of sediment gravity flows on clinoform foresets. Previous studies have created sediment gravity flows by releasing dense water-sediment mixtures into standing water, thus imposing the initial conditions for the gravity flows rather than allowing them to form on their own. Parameters such as the density, composition and initial momentum of the flows are predetermined, precluding observation of the factors that set them initially. This study uses a new experimental method that allows a range of gravity flows to self-generate. Building a clinoform using a cohesive mixture of walnut-shell sand and kaolinite allows the foreset to build up and fail episodically, generating spontaneous sediment gravity flows. Slopes undergo a series of morphological changes prior to failure, creating a concave shape that becomes exaggerated as deposition continues. This morphology leaves the slope in a metastable state. Once the slope is destabilized, failure is initiated. This study investigates the role of clinoform progradation rates on failure size and frequency. Experiments were conducted over a range of water and

sediment discharge rates. Neither failure size nor failure frequency changes with discharge rate; instead, increases in sediment supply are taken up by changes in the partitioning of sediment between the steep upper foreset and the more gradual delta-front apron below. Sediment is delivered to the delta-front apron by a form of semi-continuous slow creep along the foreset. This slow creep is a failure mode that has not received sufficient attention in the submarine mass-flow literature. The independence of failure size and frequency from sediment supply rate suggests that the presence of mass failure deposits does not provide insight on the rate of sediment delivery. If these relationships hold at field scales, this would imply that individual sediment gravity flows are relatively insensitive to changes in water and sediment supply.

INTRODUCTION

Deltaic foresets represent a critical transition from shallow-water to deep-water environments. Mass failures are believed to be the principal mode of sediment transport down marine foresets and into deep water (Kenyon et al., 1985; Wright et al., 2006; Gerber et al., 2008). The flows generated are complex and diverse in their behavior and their deposits. Most foreset mass failures are generated gravitationally and can be thought of as marine avalanches. Records of their deposits can be seen all over the world and throughout geological history (Piper et al., 2009). They have also become increasingly important as oil exploration moves into deep marine environments (Bea, 1971; Bruschi et al., 2006; Mosher et al., 2010). Submarine mass flows can also result in the destruction of underwater infrastructure (e.g., pipes, turbines, communication lines) and can generate tsunamis (Heezen et al., 1952; Tappin et al., 2001; Masson et al., 2006). Consequently, it is essential to understand the nature of these mass failures and develop a better understanding of how sediment is transported along foresets and submarine slopes generally.

Previous work on mass failures has focused on describing the morphology and deposits of these flows in ancient and modern systems. Physical experiments have been used to answer questions of the transport dynamics of these flows. Prior experimental

studies have generated mass failures by injecting slurries (a mixture of sediment and water) into ambient water (e. g., Parker et al., 1987; Postma et al., 1988; Kneller et al., 1999; Marr et al., 2001; Mohrig et al., 2003). These types of studies have provided insight on the behaviors of these flows and how they evolve over time. One limitation to these studies is that the slurries are premixed and are injected into the water column such that the initial properties of the flow -- density, composition and momentum flux -- are predetermined. This precludes observation of the processes that initiate the flows. As a result, there is a gap in our understanding of how mass failures begin and what sets their initial conditions (Piper et al., 2009).

The next step to bridging this gap is an experimental system that allows submarine mass failures to form. By allowing the flows to self-organize, we can observe how flows initiate and evolve over time. This study introduces a new method that allows subaqueous gravity flows to self-initiate and provides insight as to how sediment is transported along the foreset.

METHODOLOGY

Experimental Facility

Experiments were performed in a glass-walled flume, with a length of 12 m, width of 0.075 m and a depth of 0.30 m. In the flume, each experiment began with a pre-built ramp set to 30° and lined with gravel to prevent erosion. Sediment and water were fed using a corkscrew powder feeder and a constant-head water tank (Fig. 1.1).

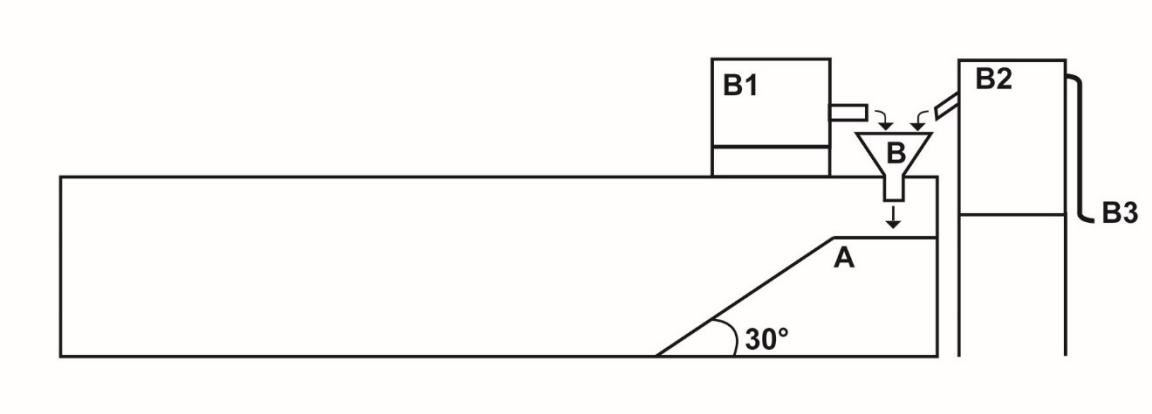

Figure 1-1 Diagram of flume setup. Experimental setup includes an initial built slope (A) of 30°, a sediment input system (B) consisting of a sediment feeder (B1) and a constant head tank (B2), where the two are mixed into a funnel and deposited down the flume. The water is fed into the head tank from a water main (B3).

Table 1-1 Summary of experiments conducted.

Run	Discharge			Failures	Normalized Failure size	Time (h:m:s)			
	Water (L/s)	Sediment (g/s)	Qs/Qw (g/L)			Duration	Failure interval	Failure duration	Frequency
1	0.021	0.94	44.76	15	0.81	1:12:03	0:02:36	0:02:12	0:04:48
2	0.007	0.94	134.28	14	0.29	1:09:31	0:03:40	0:01:23	0:04:58
3	0.03	0.94	31.33	9	0.29	1:18:44	0:07:12	0:01:05	0:08:45
4	0.036	0.61	16.94	14	0.26	1:30:13	0:05:06	0:01:04	0:06:27
5	0.03	1.28	42.66	13	0.27	1:30:22	0:05:26	0:01:29	0:06:57
6	0.023	0.61	26.52	8	0.2	1:34:59	0:08:05	0:00:56	0:11:52
7	0.016	0.61	38.12	18	0.26	1:31:32	0:03:24	0:01:13	0:05:05
8	0.008	0.51	63.75	16	0.29	1:31:32	0:05:08	0:00:47	0:05:43
9	0.012	0.78	65	8	0.33	1:31:01	0:07:50	0:01:19	0:11:23
10	0.02	0.78	39	9	0.31	1:30:01	0:06:55	0:01:16	0:10:00
11	0.027	0.78	28.88	5	0.44	1:30:02	0:13:26	0:01:30	0:18:00
12	0.028	1.11	39.64	6	0.32	1:16:08	0:10:09	0:01:08	0:12:41
13	0.019	1.11	58.42	10	0.29	1:30:01	0:07:36	0:00:48	0:09:00
14	0.011	0.83	75.45	10	0.27	1:30:01	0:06:26	0:00:49	0:09:00
15	0.01	0.98	98	10	0.3	2:52:40	0:15:53	0:01:03	0:17:16

Chapter 1

EXPERIMENTAL DESIGN

A sediment mixture of clay (kaolinite) and low-density sand-size sediment (walnut shell sand) was used. The walnut sand had a median diameter of 1 mm and a density of 1.4 g/cm^3. The basic idea was to devise a mix that, instead of producing uniform small grain flows on the foreset, as sand does, might self-organize to create larger and more complex flows that would shed light on mass-flow processes on natural delta foresets, which typically include substantial amounts of clay (Gorsline, 1984; Postma, 1984). To do this, we sought out a material that could accumulate relatively high deposit volumes and steep slopes before failing. To make sure that the clay did not simply winnow away, the walnut-shell sand was coated with dry clay to make it cohesive and allow the grains to adhere to each other. After some initial testing, a mix of low-density sand and powdered kaolinite clay was used. To uniformly coat the walnut grains, dry clay powder and walnut sand were placed in a container and was agitated. In the exploratory stages of our study, different clay to walnut sand mixtures were tested to determine an optimum ratio that would yield large and frequent failures. All experiments were conducted using this optimum ratio, 1:1 by volume. The main variables were sediment and water input rates (Table 1.1).

Data Collection

Video images were collected throughout each experiment and a frame-by-frame analysis was done to determine the precise timing, geometry, and duration of failure events. The frames before and after each failure were analyzed using a Matlab image analysis script to quantify the absolute size and shape of failure events.

FLOWS AND DEPOSITS GENERATED

The sediment gravity flows generated in our experiments were typically debris flows. The flows were generally cohesive and involved a significant fraction of plug flow

as indicated by absence of visible velocity shear. The flows were laminar and viscous-dominated. The deposits generated were generally matrix-supported and often show coarsening upward stratification, similar to mass-flow deposits seen in the field and previous experiments (Fig. 1-2) (Postma et al., 1988). Some flows generated dewatering structures after deposition (Fig. 1-2). Dewatering structures form in the toeset of the deposit, forming linear features spaced about every 5 mm (5 grain diameters). The structures form a few centimeters below the surface. As time progresses, the dewatering structures grow and eventually extended over the entire thickness of the deposit.

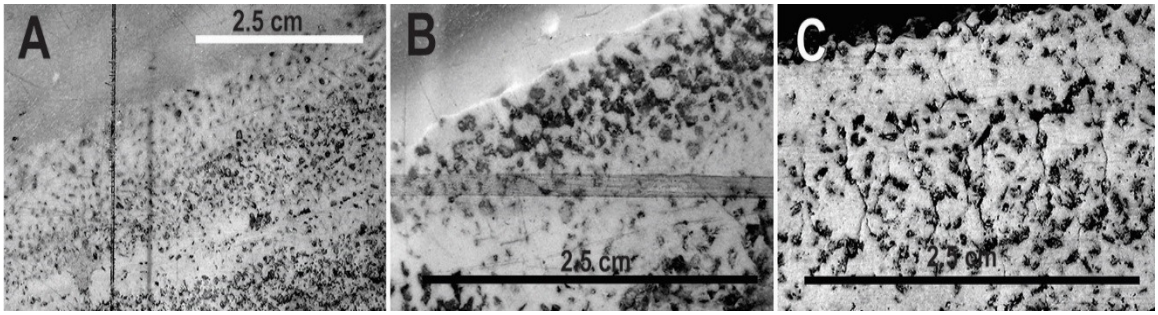

Figure 1-2 Images from the deposits generated. A. Flow in progress, flows were laminar and dominantly viscous. B. Deposits show coarsening upward stratifications. These deposits were seen at the toe of the deposit. C. Dewatering structures were observed, evenly spaced and located at the toe of the deposit.

MORPHOLOGY OF FAILURE EVENTS

Pre-failure morphology

The foreset deforms gradually, creating a sequence of morphological changes that lead to slope failure. Prior to failure, the slope develops a subtle convex shape from the knick point to the top of the delta, where knick point here means the point where there is a sharp change in slope between the toeset and foreset. This convex morphology leaves the slope in a metastable state, where slight changes in the morphology lead to slope failure. The surface starts to bulge out prior to failure, increasing the convex morphology of the slope. As the slope builds up, the shear stress on the knick point increases. Once the stress

applied is greater than some critical failure shear stress, the knick point becomes unstable and the sediment wedge begins to move. Once the sediment has been mobilized, the overlying material is no longer supported, creating headward erosion which contributes to the growing flow (Fig. 1-3 and Fig. 1-4). This process generates the sediment gravity flows. The overal shape of the clinoform profile has significantly less curvature than what is predicted by diffusional profiles (Kenyon et al., 1985).

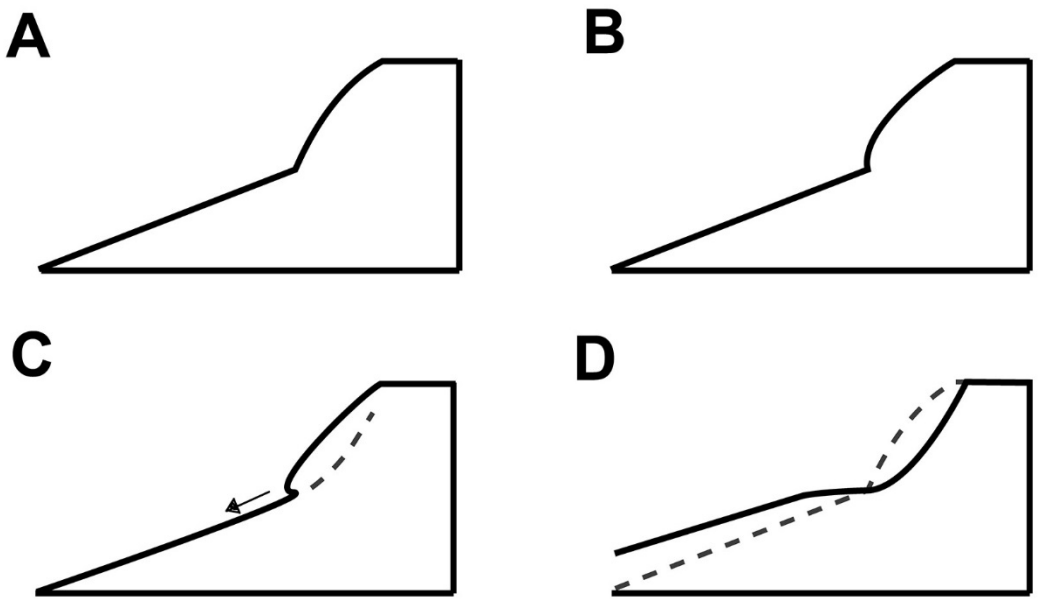

Figure 1-3 The slope undergoes a series of morphological changes prior to failure. A. Initial slope starts to form slight convex shape. B. Small shifts in the deposit form a bulging shape, increasing the stress at the knick point. C. The knick point becomes destabilized, initiating a sediment gravity flow. The material above the knick point is no longer supported, creating a domino effect. D. The material from the failure event is deposited down slope, leaving a concave scarp

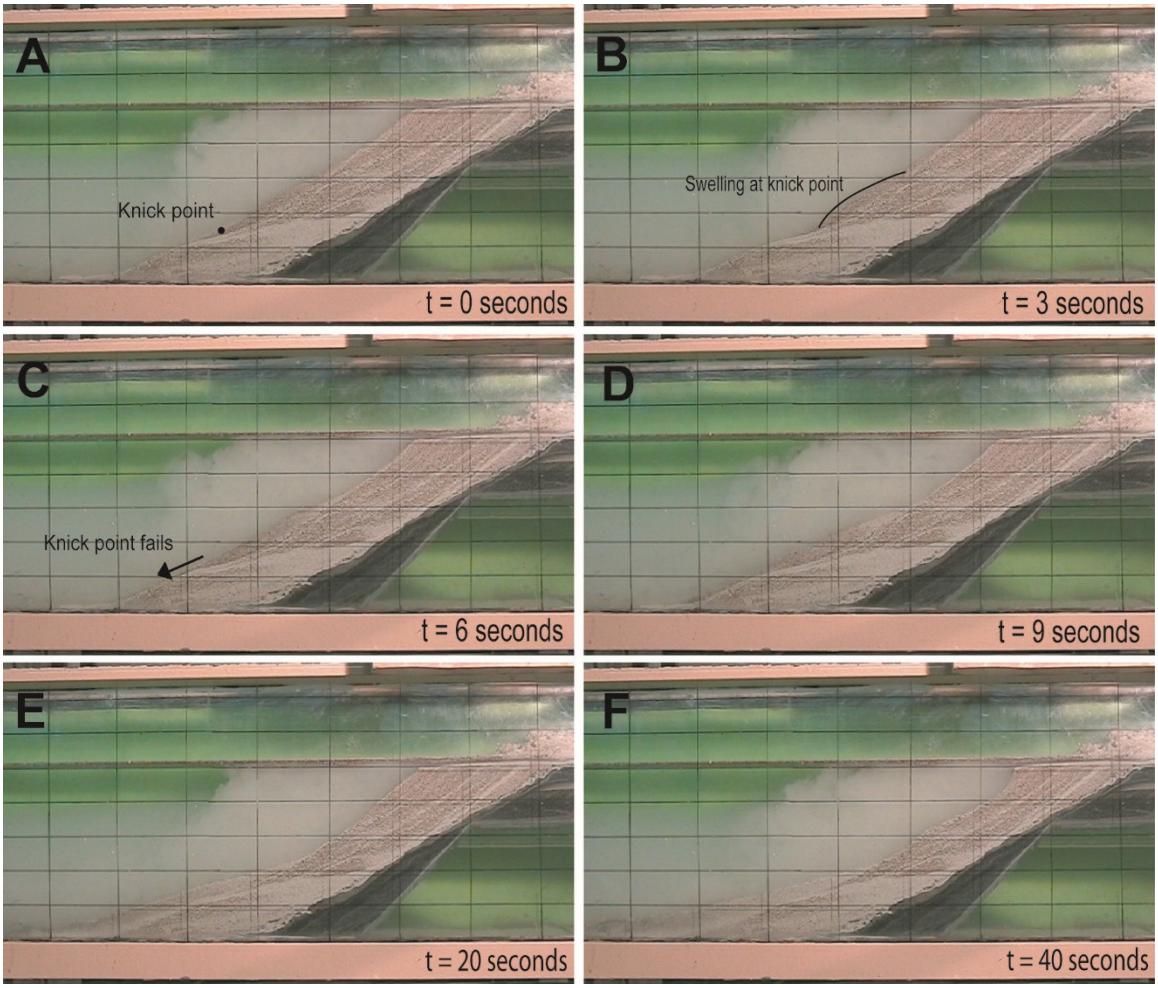

Figure 1-4 Image sequence from video of failure events which show the morphological changes which lead to failure. At 0 seconds (A), the slope starts to develop the convex morphology. At 3 seconds (B), there are slight shifts in the deposits which increases the stress on the knick point. At 6 seconds (C), the knick point fails and starts to mobilize. At 9 seconds (D), the overlying material above the knick point is no longer supported and subsequently mobilized. At 20 seconds (E), the flow is in progress. At 40 seconds (F), after the failure, the slope is left with a steep concave morphology.

Post-failure morphology

The resulting morphology after failure is a concave scarp, steeper than the initial profile. This scarp can be reactivated in future failure events. The scarp is typically back

filled by a series of grain flows. The failed sediment comes to rest as low angle deposits on the toeset, forming matrix supported, coarsening upward deposits.

THE EFFECT OF PROGRADATION RATES ON FAILURE SIZE AND FREQUENCY

One of our primary research questions was the effect of clinoform progradation rate on failure size and frequency: one would expect, for whatever failure mode dominates on the foreset, that increases in progradation rate would be accommodated by some combination of increases in failure size and/or frequency (Wolinsky et al., 2007; Kenyon et al., 1985). One would expect changes in the progradation rate to influence the size and/or frequency of failure events: previous modelling work has suggested that increases in the loading intensity from the prograding clinoform increases overpressure in the deposit, which decreases slope stability (Wolinsky, et al., 2007; Dugan et al., 2000). Thus experiments were conducted with a wide range of sediment and water discharge rates (Table 1-1). The failure geometry was measured from still images, using the methods described above, by mapping non-mobilized sediment before and after the failure. The resulting difference in sediment areas is the cross sectional area of the failure A_f, which is used to represent the size of failure events. To provide a dimensionless measure that could be compared with field cases and account for changes in water depth, the square root of the failure area A_f was normalized to the height of the foreset H as

$$\text{Normalised failure size} = A_{f*} = \frac{\sqrt{A_f}}{H} \quad (1)$$

Normalized failure sizes for individual runs and for the entire experiment are roughly normally distributed. They ranged from 0.045 to 0.588, with an average of 0.244 and a standard deviation of 0.14 (Fig. 1-5). These values fall within a range comparable to field measurements (Fig. 1-5 and Table1-2), with most values being under 1. Values greater than 1, such as the mass failure in the Bay of Bengal, were events that occurred in narrow, confined areas.

The normalized failure size is roughly constant for a range of discharge rates (water and sediment (Fig. 1-6). In particular, there is no indication that higher clinoform migration rates (higher sediment discharges) lead to larger failures. Perhaps more surprisingly, there is also no correlation between either sediment or water discharge rates and failure frequency, both independent variables had a low correlation coefficient less than 0.01(Fig. 1-7).

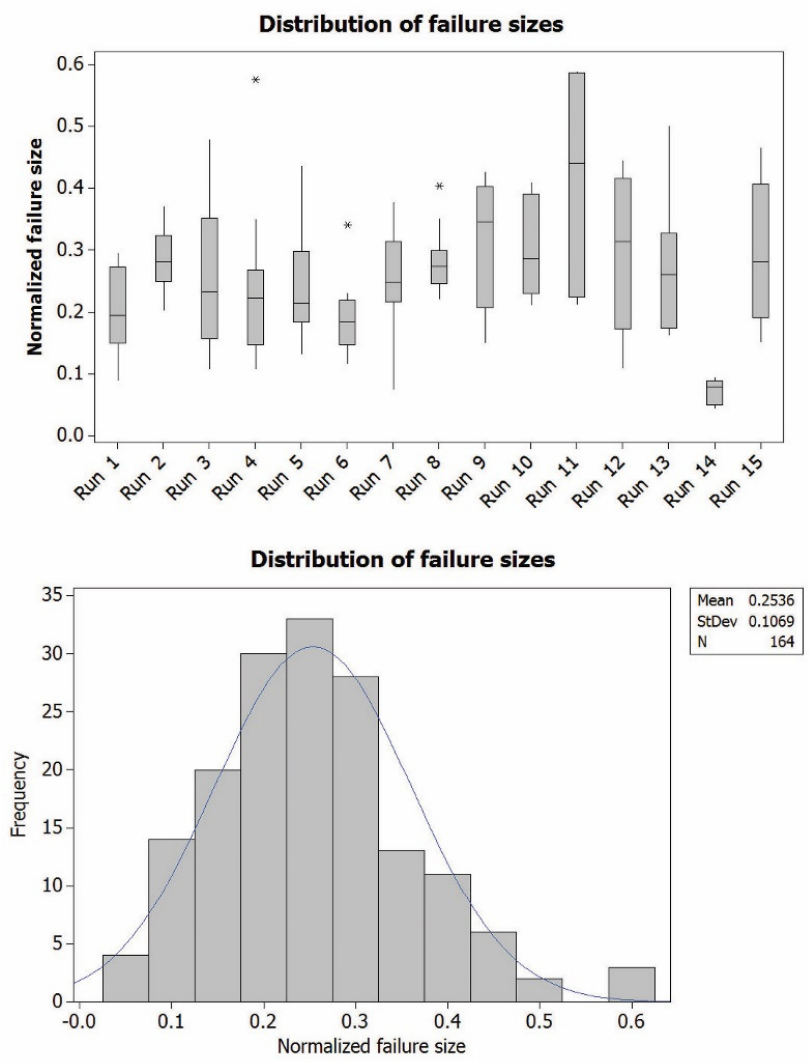

Figure 1-5 Distribution of failure sizes individually and through the entire run.

Table 1-2 Characteristics of submarine mass failures in the field

Flow	Volume (km^3)	Foreset Height (km)	Length (km)	Width (km)	Area (km^2)	Normalized failure area
Agulhas, South Africa [1,2]	20331	19.00	750	160.0	191.80	0.73
Bassein, Bay of Bengal [1,3]	900	3.00	180	37.0	24.32	1.64
Grand Banks, Newfoundland [4]	760	3.00	240	140.0	5.43	0.78
Kidnappers, New Zealand [1,5]	8	1.50	45	5.6	1.43	0.80
Papua New Guinea [1,6]	4	3.50	20	24.0	0.17	0.12
Rangers, Baja California [1,7]	12	1.25	35	8.6	1.40	0.94
Stroregga, Noreway [8]	2400	3.00	400	275.0	8.73	0.98

1. Coleman et al., 1988; 2. Dingle et al., 1985; 3. Moore et al., 1976; 4. Piper et al., 1987; 5. Barnes et al., 1991; 6. Synolakis et al., 2002; 7. Normark, 1974; 8. Haflidason et al., 2004

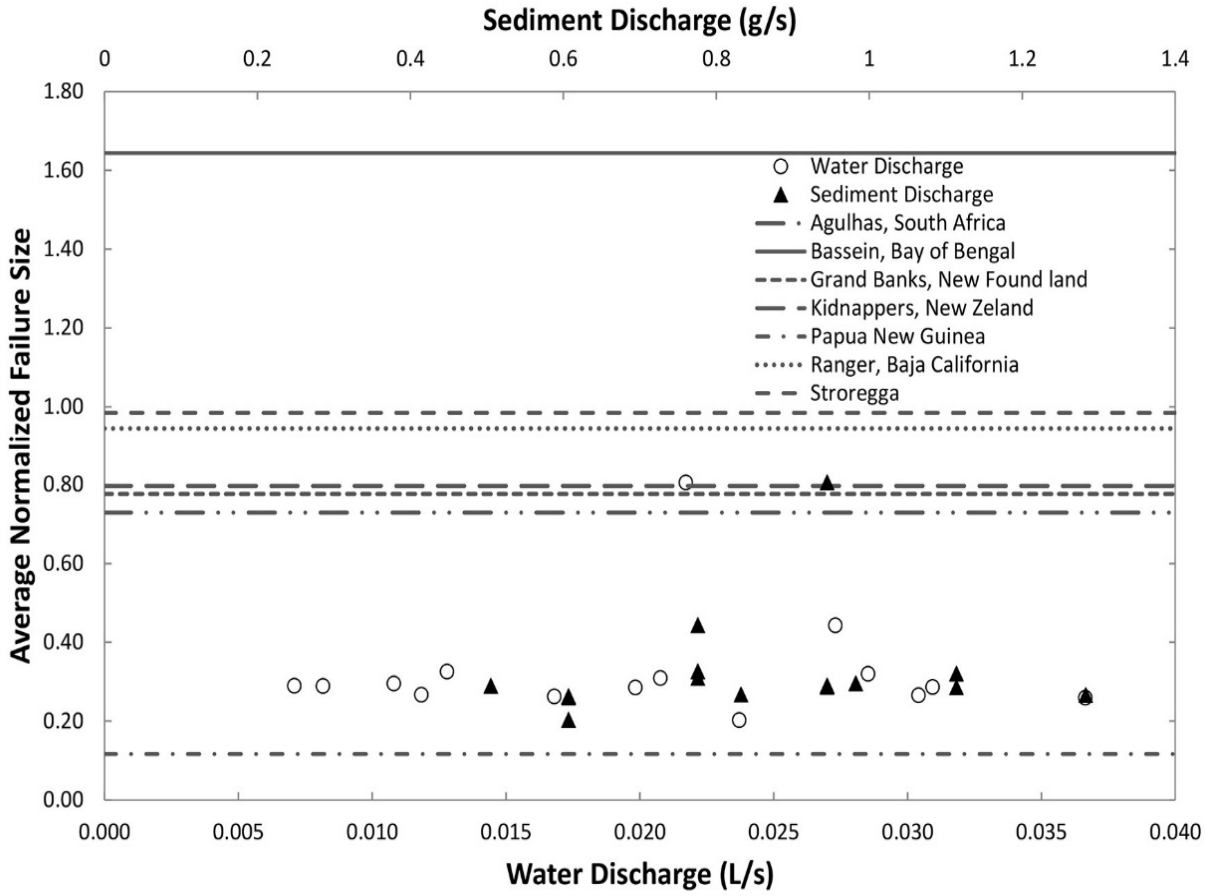

Figure 1-6 Water and sediment discharge vs. mean normalized failure size, shows that the failure size distribution is roughly constant.

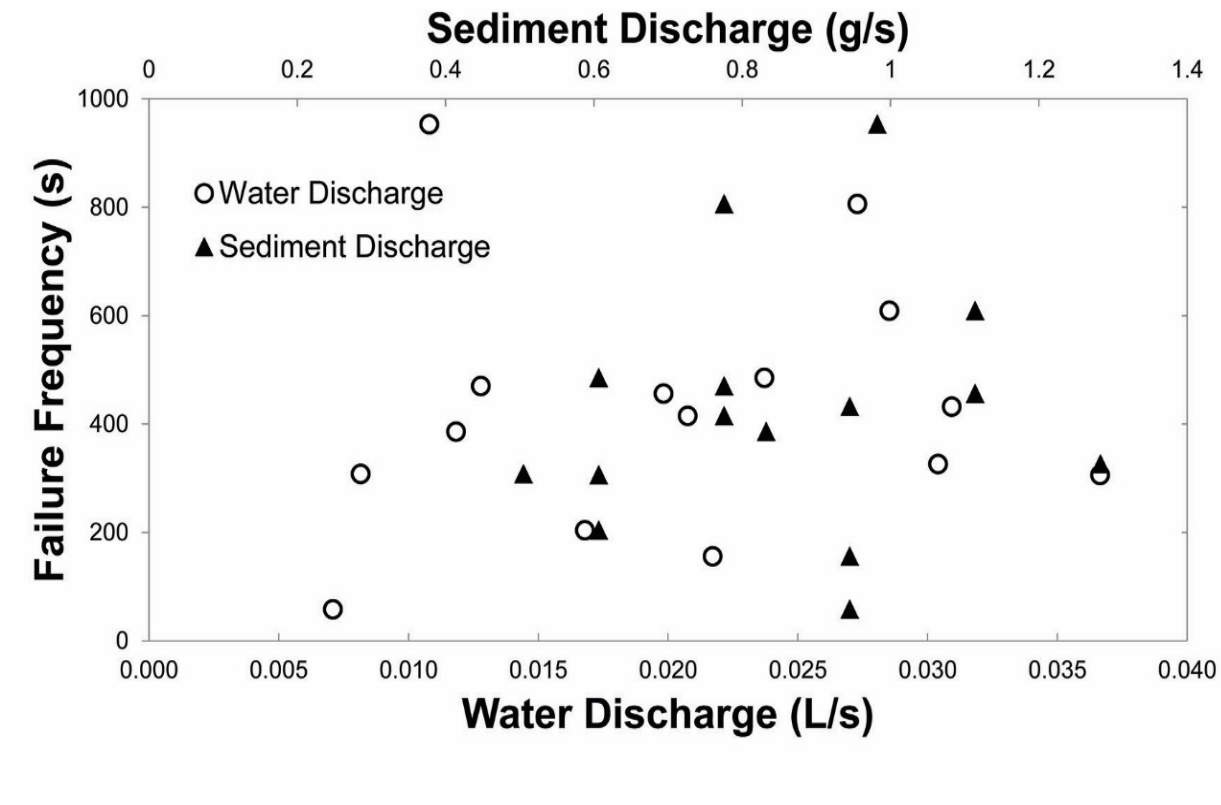

Figure 1-7 Water and sediment discharge vs. mean failure frequency, shows that there is no correlation between discharge and frequency of failure events.

CLINOFORM RESPONSE TO CHANGING DISCHARGE RATE

The apparent insensitivity of both failure size and failure frequency to changes in sediment supply poses an interesting problem: once averaged over the substantial changes in foreset geometry associated with the build-up and failure of the clinoform slope, higher sediment supply rates must (and do) lead to higher clinoform migration rates, by simple mass balance. We expected that this would be associated with an increase in either failure size or frequency, but as indicated above, this was not the case. Thus changes in the overall progradation rate must be accommodated by a different mechanism. The findings from this study suggest that increases in sediment supply are instead taken up by changes in the

partitioning of sediment between the steep upper foreset, where the failures occur, and the more gradual delta-front apron below (the delta toeset). Specifically, as the sediment concentration (Q_s/Q_w) increases, more sediment is stored in the toeset of the deposit (Fig. 1-8).

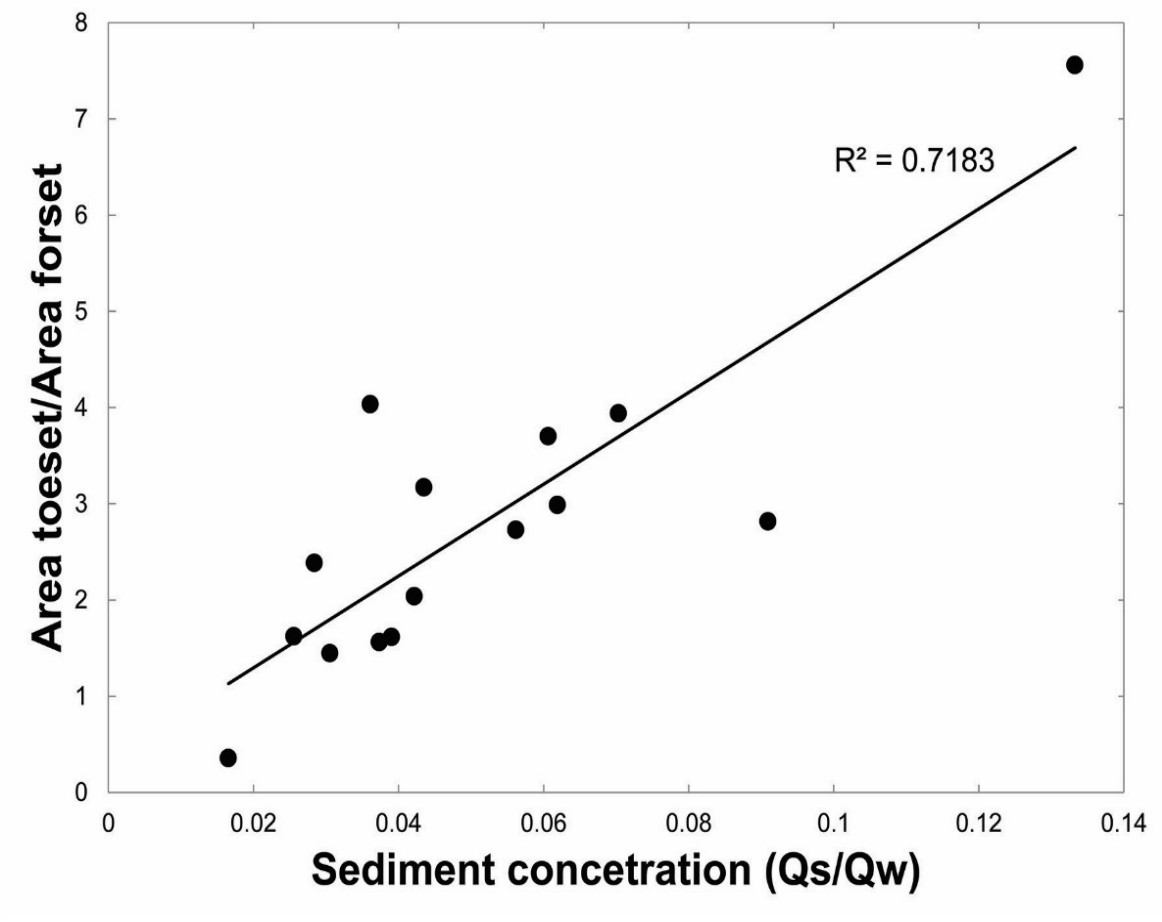

Figure 1-8 Relationship between sediment concentration (Qs/Qw) and storage partitioning (ratio of toeset to foreset area). Storage in the toeset increases with increasing sediment concentration. It is speculated that the increase of sediment placed in the toe may be the result of slow creep.

The increased sediment supply rate results in an increased level of what is defined to be background *creep*, which takes the form of semi-continuous slow sediment creep along the foreset. Sediment moved via background creep did not figure in our measurements of failure size and frequency because it did not involve distinct, measureable events, nor did it involve major changes in the geometry of the foreset surface. Thus slow

creep is considered to be an important mechanism of submarine mass flows and discuss it in more detail below.

Background creep of the foreset

The most surprising finding of our experiments is that increases in sediment supply do not create larger or more frequent discrete failure events, but are instead absorbed via background sediment mobilization in the form of a semi-continuous, slow creep of the bed. Slow creep involves the sliding of grains past each other over long time scales, with no clear distinction between frozen and flowing layers (Djaoui et al., 2005; Komatsu et al., 2001). The slow creeping of the bed takes the form of a series of micro-slumps that result from small shifts of the position of the grains. The creeping flows are 2-3 grain diameters thick and move at speeds of the order of 0.1 mm/s.

Creeping of the sediment contributes to a significant amount of progradation in the delta and has two types of transport modes: a free flowing mode and a locked up mode. In the free flowing mode, the creeping sediment slowly transports sediment to the toeset. Evidence of this mode comes from the study of changes in deposit thickness in time, where the goal is to partition the total sediment accumulation rate by rate of accumulation (Fig. 1-9). In experiments with higher sediment discharge, relatively more of the total sediment accumulation takes place in the form of gradual and continuous events (Fig. 1-9). Thus, increased sediment discharge leads to a greater fraction of creep deposits, which reduce the impact of the larger, discrete mass failure events. Total sediment accumulation is influenced more by distinct mass-failure events for lower sediment discharges compared to higher sediment discharges (Fig. 1-9). In the locked-up mode, however, sediment transported by creep processes gets stuck on the clinoform. When this sediment becomes stuck, it traps additional sediment behind it, contributing to the bulging of the sediment surface prior to failure. The only clear morphologic structure that results from these locked-up creeping flows is the bulging of the sediment at the knick point, which is a transient feature. The preservation potential for creep deposits is low and any deposit is

indistinguishable from other depositional processes, such as mass flows and grain flows (Komatsu et al., 2001).

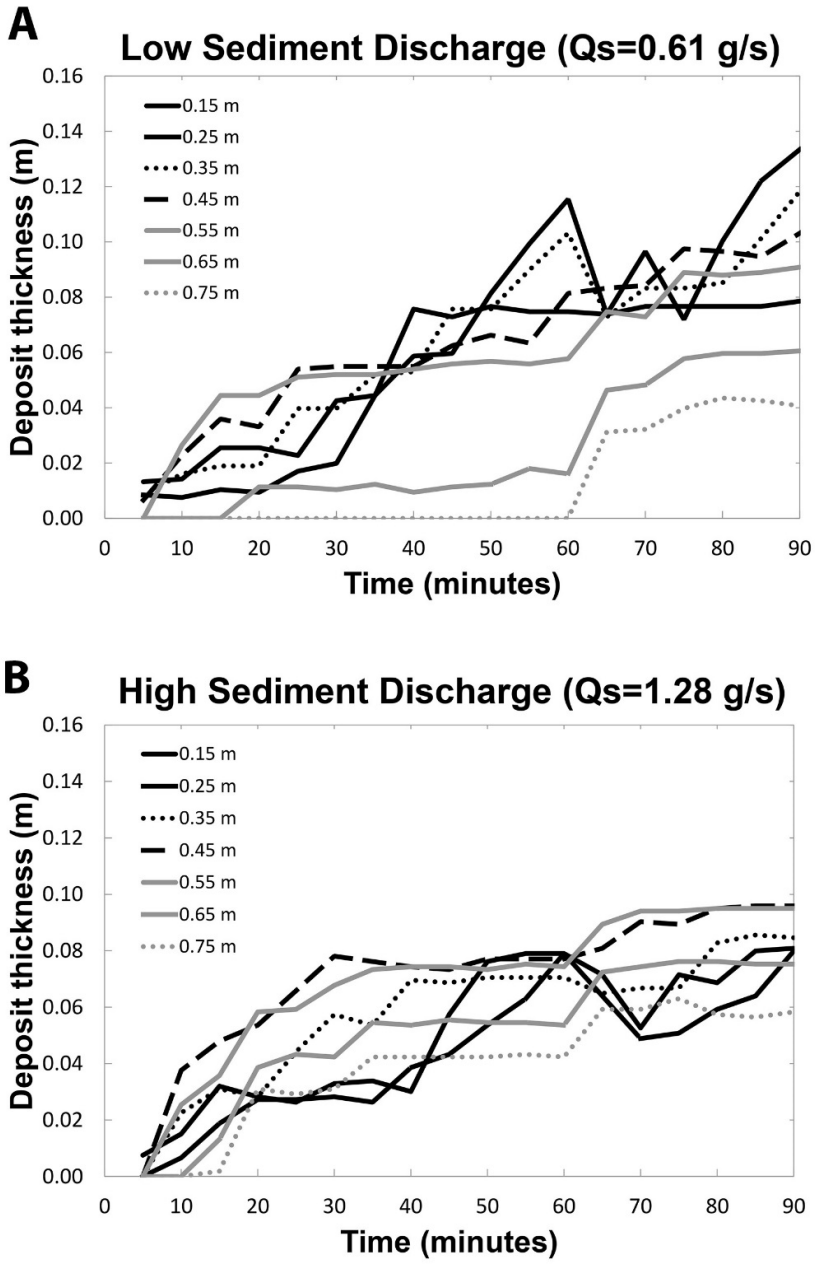

Figure 1-9 Sediment thickness through time at different distances from the feed-point. Increased sediment discharges do not contribute to larger or more frequent events, but is partitioned into background sedimentation in the form of creep. The increased rate of creep dampens the influence of failure events on the deposit.

We see no reason to think that the background-creep mechanism is an experimental artifact. However, it is a mode of sedimentation and delta progradation that has not been widely recognized in the literature. We suggest that part of the problem here is that there is generally no quantitative way to infer shear rate from preserved mass-flow deposits. Our observations did not suggest any readily recognizable difference between the creep deposits and deposits of much faster 'event-type' mass failures. Thus this suggest that deposits identified as mass-flow 'event' deposits in the field could also represent the results of slow, creeping flows. Often, it is assumed that there is an active, flowing portion of the foreset and the deposits underneath it are frozen in place. However, this supposed 'frozen' region could undergo slow, creeping flow without leaving any obvious record. Supporting evidence for the possibility of long-term slow creep in granular materials is provided by Komatsu et al., (2000), who show by analysis of images of shearing granular materials that apparently 'frozen' layers can show movement of the sediment at very low rates, when observed over sufficiently long time scales. A valuable next step would be more focused study of slow creep on subaqueous slopes to determine whether there are diagnostic structures or fabrics that can be used to distinguish creep deposits from those produced by flow modes with higher characteristic shear rates.

CONCLUSIONS

The experiments described in this paper show that:

(1) An experimental mixture of crushed walnut sand with kaolinite coating allows for development of weakly cohesive foreset slopes that generate failures of a range of size and complexity. This approach allows investigation of the processes that initiate flows and set their initial conditions and frequency.

(2) Foreset slopes undergo a characteristic set of morphological changes prior to failure, dominated by development of a distinct convex profile, which may be useful in assessing risk of failure.

(3) Neither size nor frequency of delta-front failure events increases with clinoform progradation rate. Sediment mass failures appear to have scale invariant properties, meaning that for a given input size distribution all discharges seem to produce a consistent range of small and large failures. This finding suggests that the geometry of laboratory scaled failures is insensitive to changes in sediment and water supplies.

(4) Increases in clinoform propagation rate were accommodated primarily by increases in the proportion of transport via slow creep along the foreset, which is identified as a new mode of foreset sediment transport.

(5) As sediment supply increases, the relative volume of delta-apron (toeset) to delta-foreset deposits also increases; these apron deposits represent mainly sediment moved over the foreset via slow creep.

REFERENCES

Bea, R. (1971) How sea floor slides affect offshore structures. *Oil & Gas journal*, **69**, 88-91.

Bruschi, R., Bughi, S., Spinazzé, M., Torselletti, E., and **Vitali, L.** (2006) Impact of debris flows and turbidity currents on seafloor structures. *Norwegian Journal of Geology*, **86**, 317-336.

Gerber, T., Pratson, L., Wolinsky, M., Steel, R., Mohr, J., Swenson, J. and **Paola, C**. (2008) Clinoform progradation by turbidity currents: Modeling and experiments. *Journal of Sedimentary Research*, **78**, 220-238.

Heezen, B., and **Ewing, M.** (1952) Turbidity currents and submarine slumps, and the 1929 Grand Banks Earthquake. *American Journal of Science*, **250**, 849-873.

Kenyon, P. and **Turcotte, D.** (1985) Morphology of a delta prograding by bulk sediment transport. *Geological Society of America Bulletin*, **96**, 1457-1465.

Komatsu, T., Inagaki, S., Nakagawa, N., and **Nasuno, S.** (2000) Creep motion in a granular pile exhibiting steady surface flow. *Physical Review Letters*, **86**, 1757-1760.

Marr J., Harff, P., Shanmugam, G., and **Parker, G.** (2001) Experiments on subaqueous sandy gravity flows: The role of clay and water content on flow dynamics and depositional structures. *Geological Society of America Bulletin*, 1377-1386.

Masson, D.G., Harbitz, C.B., Wynn, R.B., Pedersen, G., and **Løvholt, F.** (2006) Submarine landslides: processes, triggers and hazard prediction. *Philosophical Transactions of the Royal Society A*, **364**, 2009-2039.

Mohrig D., and **Marr, J.** (2003) Constraining the efficiency of turbidity current generation from submarine debris flows and slides using laboratory experiments. *Marine and Petroleum Geology*, **20**, 884-889.

Parker, G., Garcia, M., Fukushima, Y., and **Yu, W.** (1987) Experiments on turbidity currents over an erodible bed. *Journal of Hydraulic Research,* **25**, 123-147.

Parsons, J., Friedrichs, C., Traykovski, P., Syvitski, J., Parker, G., Puig, P., Buttles, J., and **Garcia, M.** (2007) The mechanics of marine sediment gravity flows. *International Association of Sedimentologists Special Publication,* **37**, 275-337.

Piper, D., and **Normark, W.** (2009) Processes that initiate turbidity currents and their influence on turbidites: A marine geology perspective. *Journal of Sedimentary Research*, **79**, 347-362.

Wright, L., and **Friedrichs, C.** (2006) Gravity-driven sediment transport on continental shelves: A status report. *Continental Shelf Research*, **26**, 2092-2107.

Chapter 2

2

MORPHODYNAMIC EFFECTS OF COHESIVE SEDIMENT IN EXPERIMENTAL DELTAS

SUMMARY

River deltas often have intricate and diverse shapes. The prevailing school of thought is that the wide range of morphologies observed is mainly controlled by the relative strengths of external processes (fluvial, tidal, and wave energy) acting on the system to restructure the deposit. However, it has been shown that grain size can play a significant control on geomorphic features such as planform channel morphology, which could potentially alter the behavior and morphology of deltaic depositional systems. In particular, very few studies have looked at the role of cohesion on delta morphology, where sediment under 10 μm starts to act cohesively. Here, we use three physical experiments to show that cohesion plays a strong role in setting delta morphology. We find that, holding all other factors constant, cohesive sediment alters properties including channel morphology, channel sinuosity, channel occupancy time, bar deposition, offshore slope stability, and shoreline complexity. The impact of cohesion on these geomorphic features produces differences in measured values of width to depth ratio, slope, sinuosity, bar deposition, channel occupancy time, and shoreline complexity and suggests that, consistent with numerical modeling, grain size, in particular cohesion, plays a role in determining delta morphology commensurate with that of waves and/or tides.

Chapter 2

BACKGROUND

Victor Hugo once asked how we know that "the creations of the world were not created by falling grains of sand", questioning how much of the large-scale world is determined at the smallest of scales (Hugo, 1862). When looking at systems such as deltaic deposits, it is easy to see the profoundness in Hugo's thoughts, that grains of sediment self-organize with flowing water to form these complex and diverse shapes seen across environments and though time. It is natural to wonder to what extent these shapes are controlled at the grain scale.

Geologists have long tried to understand what sets the varying patterns we see in deltaic systems. The current prevailing school of thought focuses not on grain-scale interactions, but instead on external forces acting on the system. Galloway (1975) expanded on this idea, creating a classification system to explain differing delta shapes as the result of the relative strength of fluvial, tidal, and wave forces acting on the system. While this approach clearly explains important aspects of delta morphology, it does not include any role for grain size, which various lines of evidence suggest has an important influence (Orton and Redding, 1993; Edmonds and Slingerland, 2009). In addition, the parameters for determining where a delta is located in the Galloway system are as yet not well defined. In addition, parameters such as relative fluvial, tidal and wave strength can be difficult to measure in the rock record.

While there are many who have worked on developing metrics to help provide a more quantitative approach for understanding deltaic morphology (Smart and Moruzzi, 1971; Edmonds and Slingerland, 2009; Passalacqua et al., 2013), there is no universal set of widely accepted measures of delta morphology. The Galloway classification system did not extend to include grain size until 1987 when McPherson et al. (1987) distinguished the differences between coarse-grained fan deltas and fine-grained common deltas. Orton and Redding (1993) expanded on this idea, examining different systems to determine how grain size influences geomorphic processes and features, such as channel morphology, proportion of bedload, and slope of different systems. While there have

been a few studies that have looked at the role of grain size and sediment composition, these factors have commonly been regarded as secondary in determining deltaic morphology (Edmonds and Slingerland, 2009).

Connecting back to Hugo's questions of the influence of the grain scale on the behavior of a system, we are interested here in exploring how the presence of fine-grained, cohesive sediment influences delta morphodynamics. Cohesion in the system can provide an important geomorphic threshold that previous analyses, except that of Edmonds et al. (2009), have not considered. As the numerical study of Edmonds et al. (2009) makes clear, the presence of cohesive sediment can influence factors such as slope, bank stabilization, bar formation, and channel stability, all of which should alter the large-scale morphology of a system.

One morphological difference that has been observed is that deltas with higher fractions of cohesive sediment tend to have lower gradients in their distributary networks (McPherson et al., 1987; Orton and Redding, 1993). The marine foresets of deltas with higher factions of cohesive sediment tend to have lower slopes as well (Orton et al., 1993; Pirmez et al., 1998). Thus, it appears that cohesive sediment has some influence in setting the gradient over which sediment is transported. Another morphological impact of grain size could be the stability of the deposit. It has been shown that cohesive sediment requires a higher critical shear stress to erode and entrain sediment (Orton et al., 1993; Edmonds et al., 2009; Larsen et al., 2009). This increased threshold for movement of sediment can affect the stability of banks and levees, limiting the mobility of the channel. This would allow for the banks and levees to persist over longer periods of time as well as promote the preservation of any bars which may form (Keshavarzi et al., 2005; Edmonds et al., 2009). In addition, the more persistent channels can create a concentrated jet at the river mouth that is highly erosive (Keshavarzi et al., 2005). This erosive jet can lead to the formation of sub-deltaic lobes, elongated channels, and irregular, complex shorelines (Edmonds et al., 2009).

Chapter 2

Recent numerical modeling efforts by Edmonds et al. (2009) investigated how different levels of cohesion influence the overall delta morphology, finding that the fraction of cohesive sediment in their models influenced morphological characteristics such as slope, bank stabilization, and bar formation. Their findings suggest that cohesion sets an important geomorphic threshold that could account for and create a diverse set of deltaic morphologies. For example, they found that deltas with a lower cohesive fraction had a more fan-like shape, while deltas with a higher cohesion fraction had more complex and rugose shapes. Also, they found that cohesion promoted the formation of bifurcations and allowed bars to persist.

To build upon these numerical models, here we report the results of an experiment aimed at investigating the effect of adding cohesive sediment (powdered kaolinite clay) to sand-size input sediment. The experiment was done as part of a larger series exploring delta morphology under various external forcing conditions (fluvial, tidal and wave effects, along with cohesive sediment). A controlled experiment allows us to observe and measure how the presence of clay alters the morphology and behavior of the delta. Physical experiments have often been used to understand the properties of deltas, but only a few studies have looked at the effect of cohesion on deltas (Hoyal et al., 2009; Martin et al., 2009a), as most experiments primarily focused on non-cohesive sediment (Paola et al., 2001; Kim et al., 2006; Martin et al., 2009b).

METHODOLOGY

Experimental set up

We conducted two experiments in the Delta Basin Facilities at Saint Anthony Falls Laboratory, University of Minnesota, Minneapolis, MN. The basin is a 5 m square and has a depth of 0.6 m. It has a fixed horizontal floor and water depth is maintained via a computer-controlled weir and an attached siphon in the basin (Fig. 2-1). Water and sediment are fed from a fixed point in the basin, creating an opening angle of 90°. Water is supplied by a computer-operated centrifugal pump and sediment is supplied by a cork

screw powder feeder. Sediment and water mix in a funnel and a 5 m long tubing coil to fully saturate the sediment prior to being introduced into the basin.

The basin is equipped to create experimental tides and waves to act on the delta system. Tides are created through a series of pumps to create rapid base level changes on a time scale of the order of 60 seconds, significantly shorter than the time scales on which the morphology evolves (Fig. 2-1). The pumps connect the basin to an auxiliary basin, storing water in the auxiliary basin during low tide and pumping water from the auxiliary basin during high tide. Waves are created through a floating paddle driven by a motor. The amplitude and frequency of the waves can be adjusted (Fig. 2-1), but typical values are in range of 10 mm and 1 Hz respectively.

We conducted an additional supplementary pilot experiment to highlight the morphodynamic properties of a purely cohesive (clay-only) delta. The experiment was conducted at Saint Anthony Falls Laboratory in a glass walled flume 1 m wide, 1.5 m long and 0.3 m deep (Fig. 2-2).

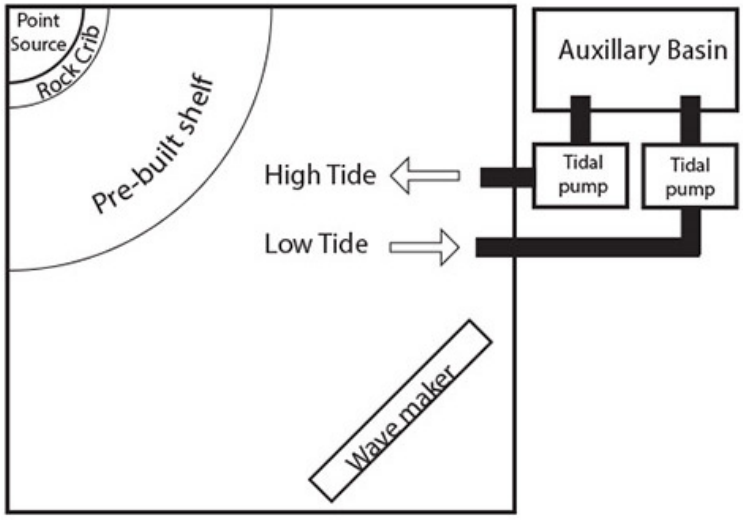

Figure 2-1 Diagram for experimental setup. Water and sediment is fed through a point source at the upper corner of the basin. Sediment is fed through a cork screw powder feeder and water is fed through a centrifugal pump. Both sediment and water are mixed together in a coil to ensure water saturation of the sediment. The delta has a pre-built shelf of sediment, made out of 100 micron sand and covered with a layer of the walnut-clay sediment mixture, to save time in the experiment. Tides are created via 2 pumps that change water level by exchanging water with an auxiliary basin. The delta basin is also equipped with a wave maker, which is a floating motorized paddle, which moves the upper portion of the water column.

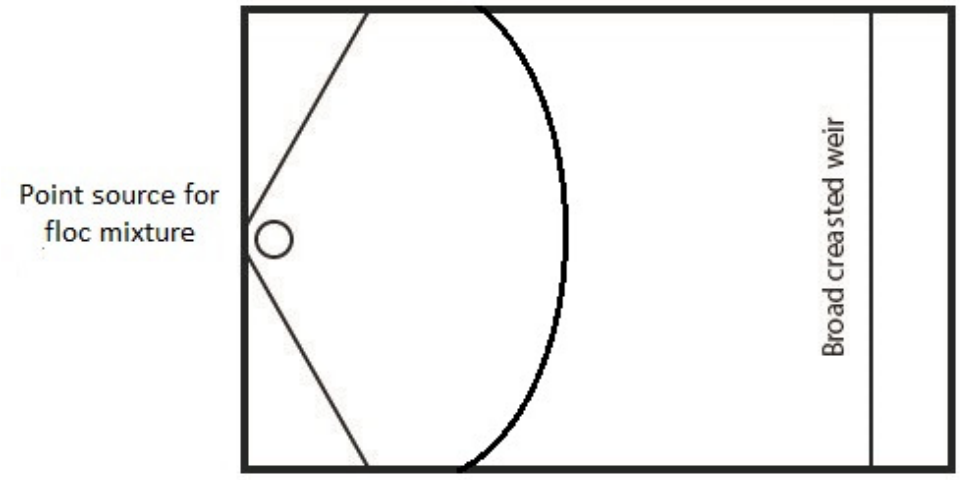

Figure 2-2 Diagram of experimental set up for supplementary clay-only experiment. A flocculated clay mixture (mix of sediment and water) was fed through a point source. The basin is 1 m by 1.5 m with a broad creasted weir of a height of 5 cm to maintain base level.

Experimental design

To explore the role of cohesive sediment in controlling delta morphodynamics under different basin regimes (fluvial, tidal, and wave dominated), we conducted two similar experiments using a constant supply of water 0.1 L/s and sediment 0.01 L/s. We maintained a constant base level of 160mm, with no subsidence. An initial platform of sediment was built (1.5 m in radius and a height of 140mm) to expedite the experiment.

The main difference between the two experiments was the sediment types used, a non-cohesive and cohesive sediment. The non-cohesive sediment was a well sorted walnut-shell sand with a median grain size of 1 mm. The cohesive sediment was a 1:1 mix by volume of the same walnut sand and dry powdered kaolinite clay. Previous experimental work has shown that the addition of clay expands the range of foreset dynamics to include large, intermittent failure events as compared to the fairly regular, small avalanches that are characteristic of non-cohesive flows (Abeyta and Paola, 2014). Details of each experimental run are described in Table 2-1. We compare experimental results after the same volume of sediment has been delivered to the basin under a given condition (e.g., fluvial, tides, and waves).

The sediment used in the supplemental experiment was flocculated kaolinte clay sediment with a median grain size of 0.3 mm and a density of 1050 Kg/m^3 (properties reported are for flocs, not individual grains that make up the flocs). Our reasoning for using flocculated clay sediment is that flocculation dramatically alters the transport properties of cohesive sediment; without flocculation the experiment would have not developed a transport slope and the clay would have stayed in suspension (Schieber et al., 2007; Schieber and Southard, 2009-a; Schieber and Yawar, 2009). The clay was flocculated by mixing clay with chemical flocculants (2kg of clay per 40L of flocculent mix), a combination of an industrial polymer Superfloc (500 µL/L of water) and iron chloride (6 g/L of water). The floc mix (flocs + water) was hand fed at a rate of 0.006 L/s from a point source, opening into an angle of 160 degrees at a constant water depth of 3 cm. The supplemental experiment was significantly shorter than the main runs due to high rates of compaction of the deposit, and the availability of flocculating chemicals.

Table 2-1 Summary of run parameters

	Cohesive	**Non-Cohesive**	
	Run hours	*Run hours*	*Procedure*
Fluvial	0 - 100	0 - 80	No waves or tides
Tidal	100 - 145	80 - 120	Amplitude = 10mm, Frequency = 1 minutes
Wave	145 - 195	120 - 160	1 wave per second

Data collected

Overhead photos of the delta basin experiment were taken every 30 seconds. We used these images to map and measure morphological changes in the delta through time. High-resolution laser topography was also collected every 10 hours. In the supplementary experiment, high-resolution video was recorded through the flume sidewall and laser topography was collected at the end of the experiment.

Measurements

Width to depth ratio

We collected a series of 10 cross sections from each high-resolution topographic scan, equally spaced along the channel. The distance between the top of each bank was defined as the width of the channel, and the vertical distance between the banks and the thalweg was defined as the channel depth. We report the mean value of the width: depth ratio for a given hour.

Slope

We collected three long profiles from each high-resolution topographic scan. The first long profile collected was along the centerline of the channel to define the channel slope. The last two long profiles were collected on either side of the channel to determine topset slope, and we report the average of the two long profiles obtained in this way.

Sinuosity

Channel sinuosity is defined as the ratio of channel length to valley length. In this experiment, we measured the length of the channel along the centerline. The distance between end points, from apex to shoreline, was defined as the valley length.

Bars

We measured and mapped bar deposits on the delta at one hour intervals. For this analysis, we define a bar as a depositional feature that horiztontally deflects the flow in the channel. We further break this down to three subtypes of bars: mouth bars, scroll bars, and channel bars. A mouth bar is defined as a depositional feature that is formed at the shoreline and that bifurcates the flow. A scroll bar is defined as a depositional feature that is formed as the result of lateral migration of the channel. A channel bar is defined as a depositional feature that forms in the center of a channel. Aspect ratio was collected on all bars, and is defined as the ratio of the longest downstream length to the widest cross stream width. Bifurcation angle was measured by the angle of intersection of a line of best fit on either side of the bar that points upstream.

Channel occupancy

We used three different metrics for channel occupancy time. The first metric was the measured number of hours a channel stayed in a position. These measured values

were averaged over a given experimental phase. The second metric was water occupancy maps, which measured the percentage of experimental time that water occupied a given area. This was done by creating land-water maps, where for an RGB digital image, the red band of the image was divided by the blue band to increase the contrast between land and water. At one hour intervals, the images were summed to count the number of times water occupied a given pixel. The last metric used was change in water surface, where the sum of pixels containing water was normalized by the total area of the delta topset. The derivative of this ratio was used to measure the change in water on the delta surface through time.

Shoreline complexity

Shoreline complexity is measured here by using the *area-deficit ratio*: the ratio of area of the actual delta topset to the area of the convex hull of the delta topset (Fig. 2-3). The closer the ratio is to one, the simpler the shape is.

OBSERVATIONS AND INTERPRETATIONS

Channel Dynamics

Channel morphology

At first glance, the channels in the non-cohesive system tended to be broad and uniform as compared to the channels in the cohesive system, which tended to be narrow and variable in shape. Looking at the hydraulic geometry (Fig. 2-4), the channels in the cohesive delta tended to have a well-defined thalweg, scours and a well-developed flood plain. Channel width: depth ratios in general were consistently significantly lower in the cohesive systems (Table 2-2).

Adding tides increased the channel width: depth ratio in the non-cohesive system but decreased the width: depth ratio in the cohesive system. The difference in behavior is the result of different critical shear stresses required to remobilize sediment, which allows the tides to rework the channels more readily in the non-cohesive system. When compared to the fluvial dominated phase, adding waves decreased channel width : depth ratios in both systems.

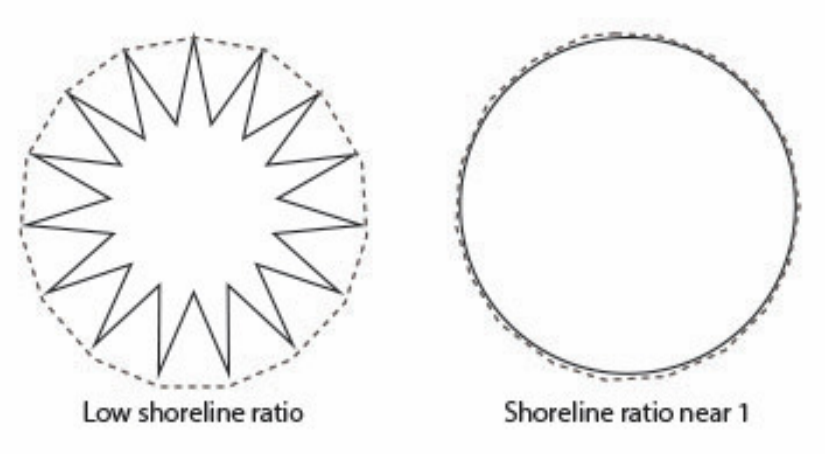

Figure 2-3 Example of shoreline complexity measurmeents. To quantify shoreline complexity, we use the ratio of the measured area of the object to the area of the convex hull surrounding the object (area-deficit ratio).

Table 2-2 Summary of Width to depth ratios, averaged for a given experimental phase.

Width to depth ratio		
	Cohesive	*Non-cohesive*
Fluvial	21.0	34.0
Tidal	18.9	35.6
Wave	18.4	27.7

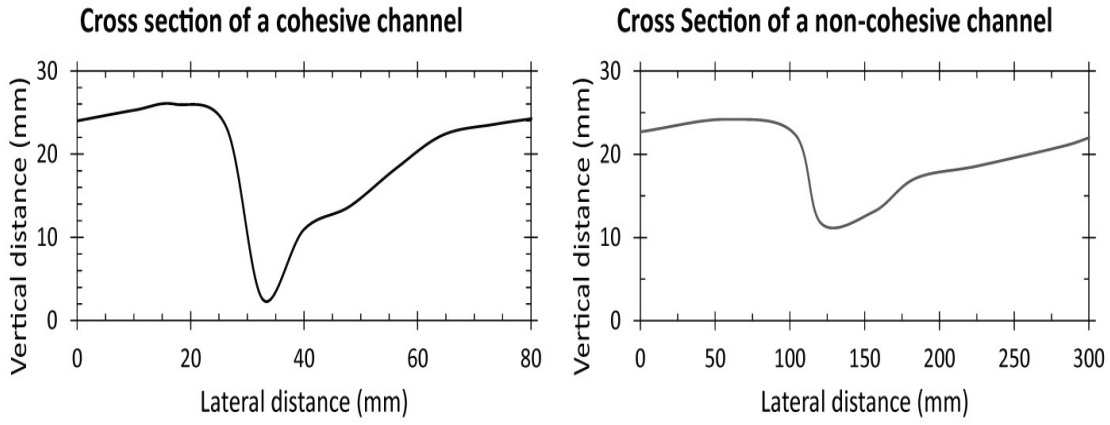

Figure 2-4 Comparison of representative two cross sections of channels in both the cohesive and non-cohesive system. The cohesive system shows greater variablity in morphology with a well defined thawleg as the non-cohesive systemm tends to be broader and shallower.

Channel slopes

The transport slopes in both experimental series reported here were in general lower than for common mixes used for experimental deltas, which are typically dominated by quartz sand; the reduction was about 0.03 degrees (Table 2-3). Overall, the transport slopes in the channel were comparable between the non-cohesive and cohesive system under fluvial conditions. Under tidal conditions, the non-cohesive system became steeper (Table 2-3). The increase in slope is the result of the tide reworking the sediment at the mouth of the river and the transport slope then adjusting to this change in sediment flux (Chapter 3). The cohesive system saw a reduction of slope under tidal conditions. Under wave conditions, both the cohesive and non-cohesive systems had an increase in transport slope, which appears to be the result of the reworking of the shoreline and the damming of the fluvial system with beach deposits (Table 2-3).

Table 2-3 Summary of slopes measured, reported here is the average slope for a given phase, measured in mm/mm. Traditional mixes are the commonly used quartz sand and coal mixes

Channel and topset slope

	Cohesive		***Non-cohesive***		***Traditional mixes***	
	Channel	*Bank*	*channel*	*bank*	*Channel*	*Bank*
Average	0.011	0.021	0.012	0.017	0.057	0.072
Fluvial	0.009	0.019	0.010	0.017		
Tidal	0.008	0.021	0.013	0.016		
Wave	0.016	0.022	0.014	0.018		

Channel Sinuosity

The sinuosity values measured in our experimental systems typically fell in the range from 1 to 2, within the range of values found in natural systems (Fig. 2-5, Leopold et al., 1964; Mueller, 1968). Overall, the cohesive system had higher sinuosity values (average of 1.56, standard deviation of 0.15 for cohesive systems compared to average of 1.46, standard deviation of 0.15 for non-cohesive systems), consistent with meandering rivers at field scales (Fig. 2-5). The non-cohesive sinuosity values were in general lower and fell slightly below the 1.5 threshold for river meandering. It is important to note that the 1.5 threshold defined for sinuous channels is somewhat arbitrary and does not

represent a clear threshold in any physical properties in the channel. The lower critical shear stress and lower bank strength of the non-cohesive system allow the channel to migrate laterally more readily, and to create new, straighter pathways, which likely accounts for the lower sinuosity values.

The tidally dominated portion of the experiment for both systems produced the most sinuous channels with the lowest variation in channel sinuosity (Fig. 2-5). While there has not been a comprehensive study on bulk channel sinuosity distributions across delta types, some speculate that tidal channels in the field tend to have high sinuosity values (Gastaldo et al., 2009) while others did not find a significant difference between tidal and non-tidal channels (Bain, 2014). Fluvial- and wave-dominated experimental deltas produced comparable channel sinuosity values, but the variation in channel sinuosity was much lower for the wave-dominated systems (Fig. 2-5).

Channel mobility

Channels, as defined by the presence of relatively deep water on the surface, remained in place over significantly longer time scales (around 5 times longer) on the cohesive delta and had longer channel occupancy times (Fig. 2-6). When looking at wetness maps of the deltas over the length of each phase of the experiment, it is clear that the channels in the cohesive system developed preferred and long-lasting paths, and that the non-cohesive system tended to have a more dispersed distribution of water on the surface. The increase in channel occupancy time and increased channelization are largely due to the reduced ability to re-erode previously deposited sediment. In the presence of cohesion, sediment sets up over time such that deposited sediment requires a much higher critical shear stress to remobilize compared to what it took to keep it in transport. As a result, the levees become more stable, limiting the amount of lateral channel migration that can occur. Also, the influence of offshore events contributed to the formation of migrating knick points that caused the cohesive system to form deep incised channels, which were not observed in the non-cohesive system (Chapter 3). The resultant deep channels made it difficult for water to breach the levees and avulse.

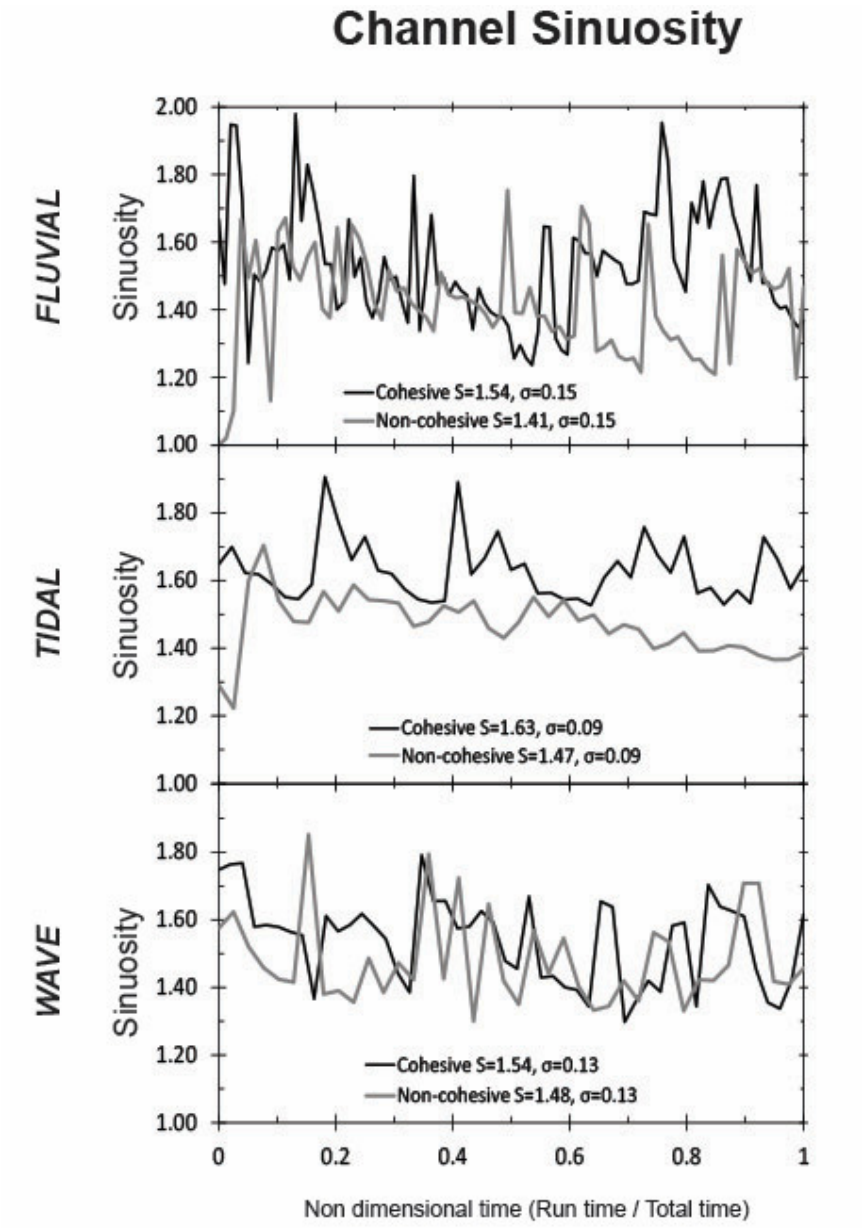

Figure 2-5 Measures of channel sinuosity through time with respective averages (*S*) and standard deviations (α) reported for each system.

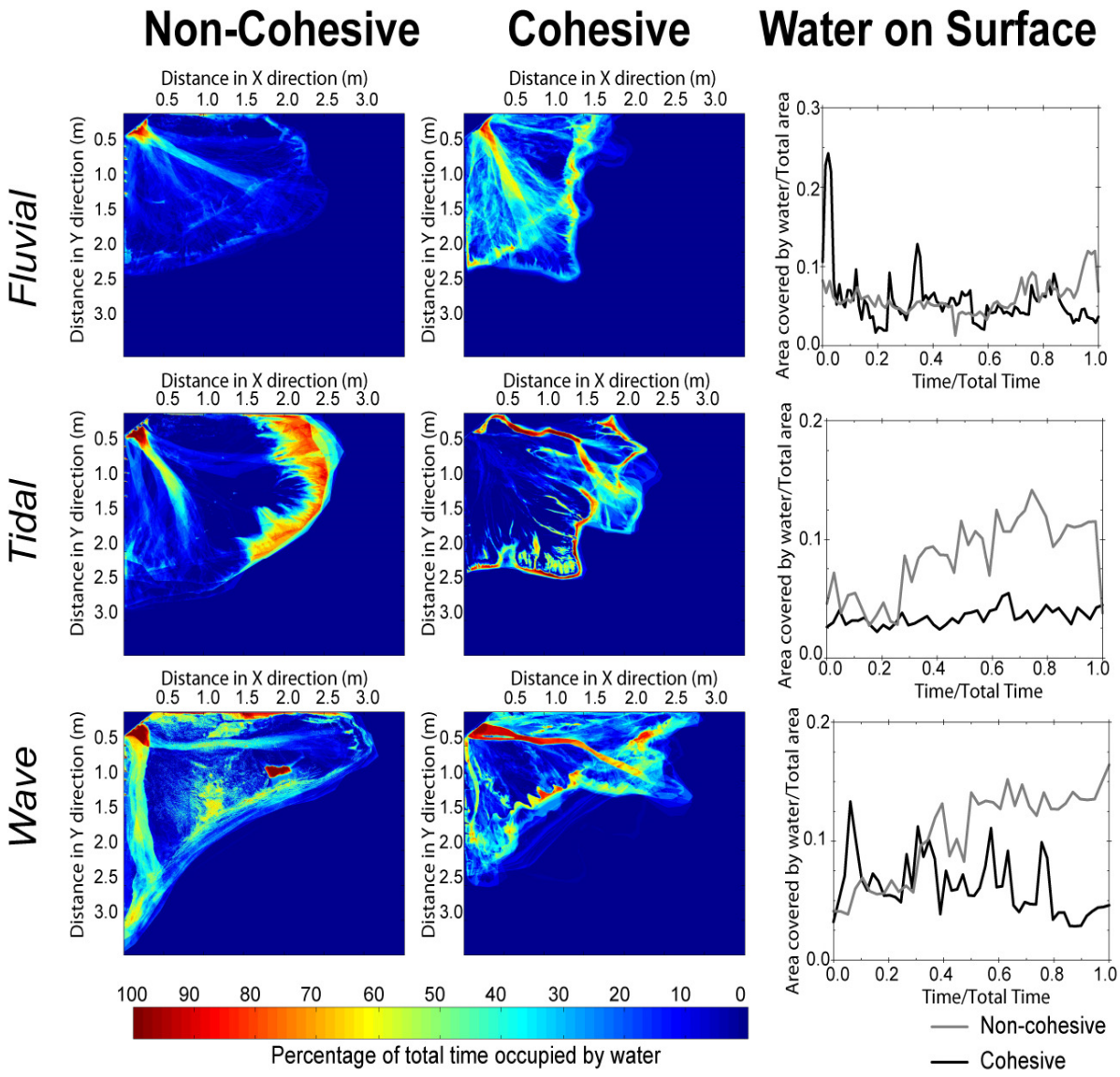

Figure 2-6 Channel occupancy time and time evolution of water on the surface. Channel occupancy maps are created by measuring the total number of images that contain water at a given pixel location. We then use this information to measure changes of water on the delta surface through time.

Interestingly though, the purely cohesive (clay-only) delta behaved more similarly to the non-cohesive system. The flocculated clay sediment was moved and transported as bedload material and behaved similar to the non-cohesive system – a behavior also observed in experimental work by Schieber et al. (2007, 2009). The flow on the surface of the floc delta was dominantly sheet flow, forming only weak, short-lived channel systems. This behavior is closer to that of previous experiments that used coarse quartz sand (e.g., Paola et al., 2001).

The observation of longer channel occupancy times holds true regardless of the dominant process (waves, rivers, or tides) acting on the basin, with cohesive sediment producing significantly longer time scales (Fig. 2-6). Fluvially dominated deltas produced the most active channels with the shortest channel occupancy time (Fig. 2-6). Tidally dominated deltas had significantly more stable channels with high occupancy times, with or without cohesive sediment, which suggests that the tides stabilize the channels (Fig. 2-6); adding cohesion amplifies this effect. This observation is aligned with field observations, which show that tidal channels on deltas do not migrate much, if at all (Leven, 1995; Fargherazzi et al., 2004). Wave-dominated deltas also show an increase in channel occupancy time, and even though the effect is not as dramatic as in the tidal case, this observation also suggests that waves act to reduce channel mobility (Fig. 2-6).

Avulsion style

The way the channels avulsed differed significantly between the cohesive and non-cohesive systems. In the non-cohesive system, the channels tended to sweep across the surface of the delta, migrating laterally as the channel gradually changed position over time. This observation can be seen through the wetness maps, which show a more diffused distribution of water across the delta surface (Fig. 2-6). In contrast, the cohesive deltas did not migrate gradually across the delta but rather abruptly changed channel position, i.e. avulsed. Prior to avulsion in the cohesive system, the channel gradually became shallower through backfilling (Hoyal and Sheets, 2009). As the channel became shallow enough, the entire surface flooded and the water began searching for a new path,

typically occupying previously existing paths. This is seen when looking at the changes in surface water on the delta over time, where the cohesive system has rapid and abrupt pulses of water covering the delta while wet fraction in the non-cohesive system showed low amounts of changes in the wet fraction (Fig. 2-6).

Bars and bifurcations

Formation of bars

The presence of cohesive sediment significantly alters the rate of bar formation, regardless of the dominant external influence acting on the system. Averaged over the entire experiment, the cohesive delta produced around 1.4 bars/hour as compared to the 0.7 bars/hour for the non-cohesive counterpart (Fig. 2-7 and Table 2-4). This observation is consistent with current numerical models, which predict lower rates of bar formation for non-cohesive systems as bars formed in this system would not have internal strength to maintain and preserve the bars (Edmonds and Slingerland, 2009). Thus, by adding fines and cohesion to the system, the bars develop internal strength that increases their chance for survival, development and preservation (Keshavarzi et al., 2005; Edmonds and Slingerland, 2009; Larsen et al., 2009).

When compared to fluvial conditions, the addition of waves or tides to a system reduced the occurrence of the bars, as their action tends to remove and rework the sediment in the system (Fig. 2-7 and Table 2-4). Tides were the greatest hindrance to the formation and preservation of bars, which suggests that the bidirectional flows were effective at reworking and preventing sediment deposition within the channel system (Fig. 2-7 and Table 2-4). Waves, despite having the greatest capacity in our experiments to rework and reshape the entire shoreline, did not reduce frequency of bar occurrence to the extent that tides did (Fig. 2-7 and Table 2-4).

Type of bars formed

Of the types of bars produced, mouth bars were the most frequent in both systems (Fig. 2-8). For the cohesive case, scroll bars were more frequent relative to mid-channel bars as the channels produced are more sinuous and migrated laterally to form scroll bars

(Fig. 2-8). For the non-cohesive case, scroll bars and mid channel bars occurred at comparable rates (Fig. 2-8).

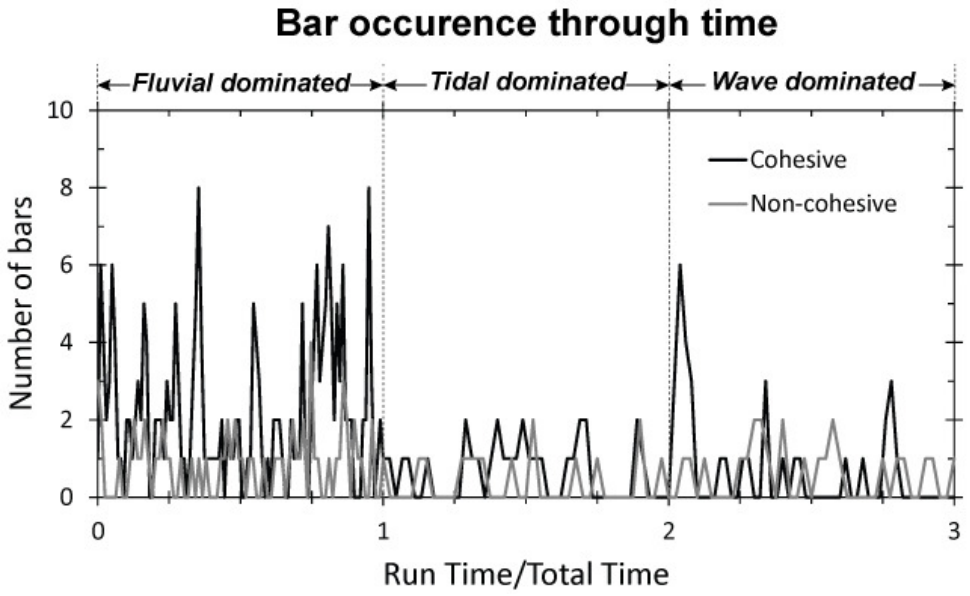

Figure 2-7 The total number of bars observed during different expeirmental phases.

Table 2-4 Number of observed bars by sediment type and external forcing.

Bar Summary			
		Cohesive	*Non-cohesive*
Summary	Entire Run	296	105
	Fluvial	221	67
	Tidal	28	14
	Wave	20	24
Fluvial	Mouth	97	38
	Meander	89	13
	Scroll bar	35	16
Tidal	Mouth	6	3
	Meander	18	9
	Scroll bar	4	2
Wave	Mouth	11	5
	Meander	5	7
	Scroll bar	4	12

Under fluvial conditions, mouth bars were the most frequent regardless of the dominant sediment type (Fig. 2-8). This is because the fluvial dominated case did not have external influences acting along the shoreline that remove and rework sediment, i.e. tides and waves. As a result, the survivability and preservation potential for mouth bars increased dramatically for fluvial conditions. Mouth bars were the least frequent under tidal conditions, which suggests that the tides remobilize sediment at the river mouth.

Under tidal conditions, scroll bars were the dominant type of bar formed for both sediment types (Fig. 2-8). This is because channel mobility dramatically decreased as tides stabilized the channel position. Any migration of the channel was through incremental lateral migration that left scroll bars along the channel.

The occurrence of mid-channel bars was comparable for both fluvial and wave conditions for both sediment types, with a decrease in formation under tidal conditions (Fig. 2-8). The decrease in frequency suggests that tides have a stronger upstream influence on channel flow dynamics and sediment deposition compared to fluvial and wave conditions.

Morphology of bars

Overall, non-cohesive systems produced bars with a larger median size under all conditions. The distributions for bar sizes for the non-cohesive system tended to be broader as the non-cohesive system produced distributions that were skewed toward small sizes (Fig. 2-9). The cohesive system also produced the largest bars recorded, however there were very few of these large bars. In general, bars formed under fluvial conditions were larger than those formed under wave conditions for both the cohesive and non-cohesive cases, which suggests that external effects such as waves limit bar size, even away from the shoreline. For the cohesive system, tides produced the smallest bars, however tides produced the largest bars for the non-cohesive system (Fig. 2-9). This suggests that the sediment type has its strongest influence on bar size under tidal conditions.

The aspect ratios for bars in the cohesive delta tended to be higher, producing longer and narrower bars than the non-cohesive delta. The largest difference in aspect ratio is seen under fluvial conditions, which suggests that sediment type has more influence on bar morphology under fluvial conditions than with wave or tide influence (Fig. 2-10). However, the bar aspect ratios for cohesive vs. non-cohesive sediment under tidal and wave conditions are very similar to each other, with tides producing bars with higher aspect ratios with or without cohesion. The similarity in trend suggests that the external effects (tides and waves) set the aspect ratio for bars, rather than sediment type.

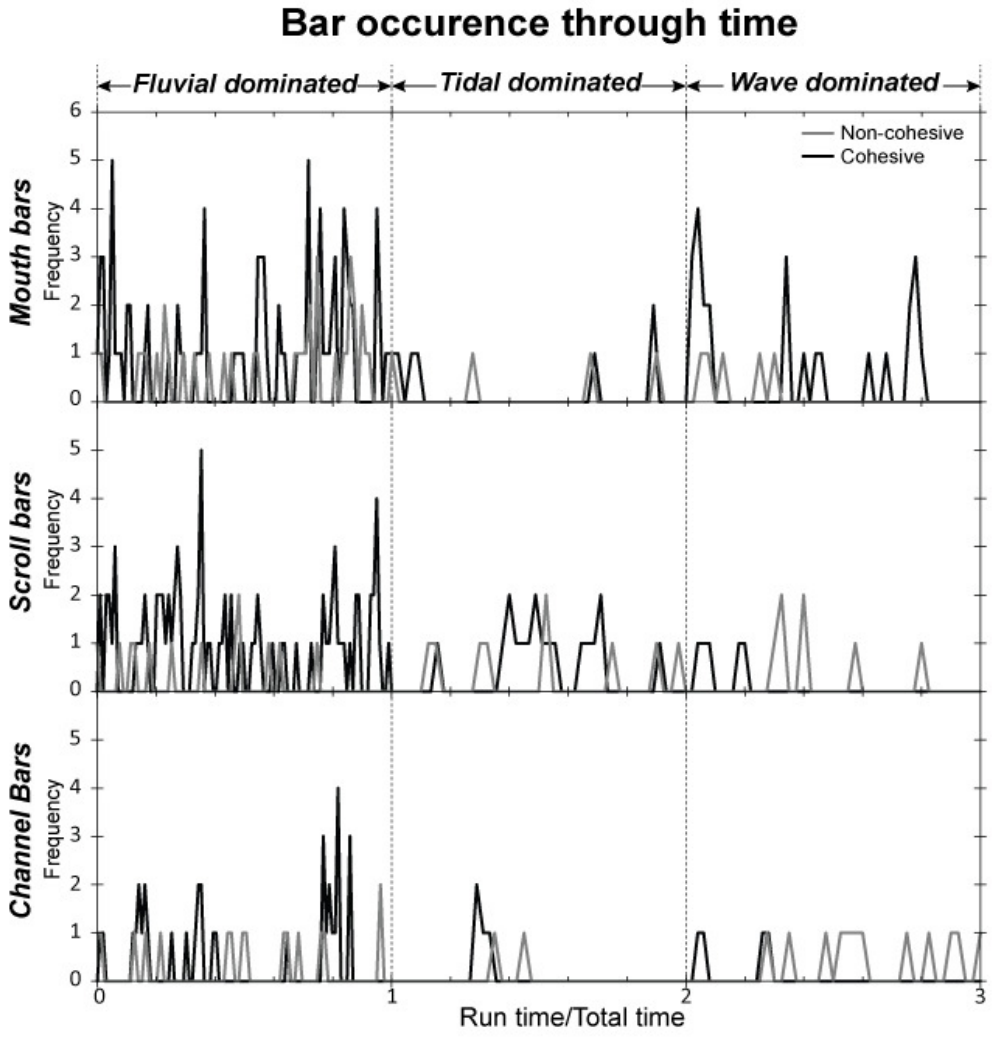

Figure 2-8 The occurance of different types of bars through different experimental phases.

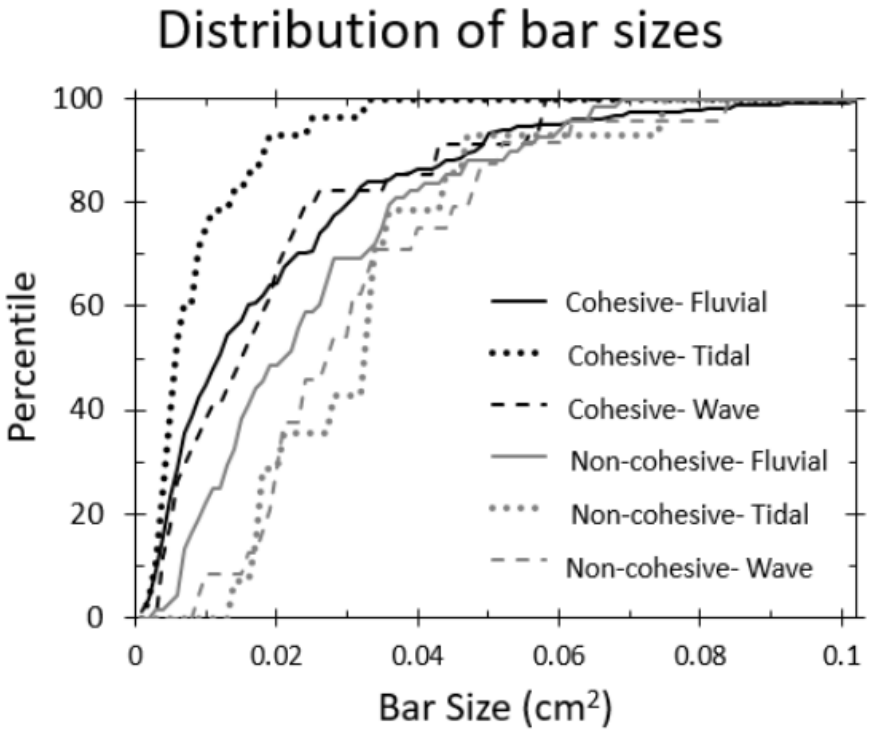

Figure 2-9 The size distributions of bars

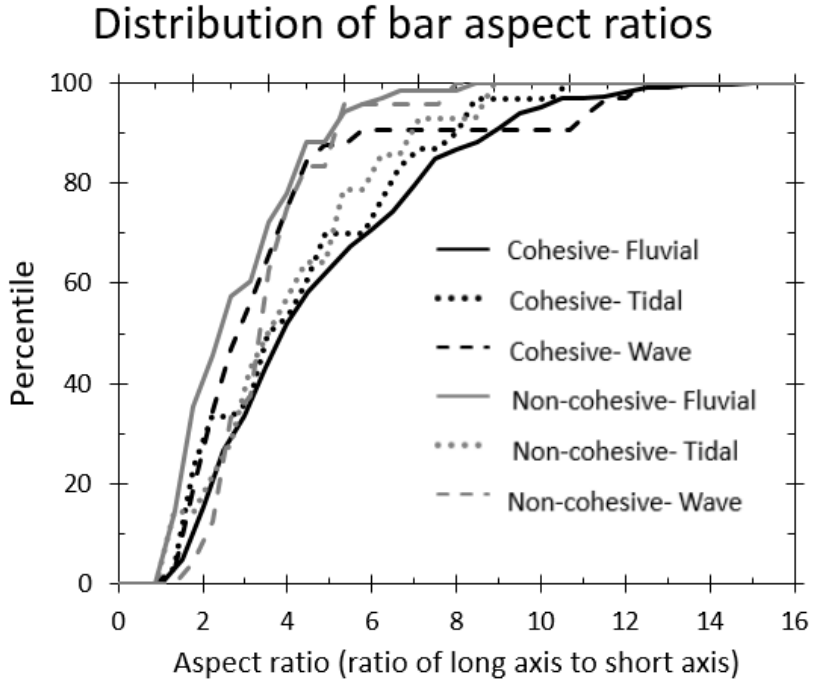

Figure 2-10 Distribution of aspect (length:width) ratios

Another morphological aspect we looked into was the bifurcation angle for channel mouth bars. Averaged over the entire experiment, non-cohesive bars bifurcated the flow at higher angles under all conditions, by an average of 20° (Table 2-5). Tides for both systems produced the largest bifurcation angles due to the bidirectional flow that spreads and disperses sediment deposited on the mouth bar (Table 2-5). Waves produced the lowest bifurcation angles, which suggests that unlike tides, waves do not smear the mouth-bar sediment to produce larger angles. While the sediment type seems to set the scale of the bifurcation angle, waves and tides have a consistent influence on it.

Table 2-5 Summary of opening angles of mouth bar deposits

Mouth Bar opening angle		
	Cohesive	*Non-Cohesive*
All	35.8	49.9
Fluvial	36.8	50.3
Tidal	40.2	65.7
Wave	24.4	37.2

Offshore behavior

One distinct difference between the cohesive and non-cohesive system is the role of offshore behavior in the overall dynamics: the cohesive system produced a wider range of the behaviors observed in natural systems, in particular, that of mass failures. The addition of cohesive sediment has been shown to alter foreset mass flow dynamics away from the fairly regular small avalanches characteristic of cohesionless grain flows to a range of mass failures including intermittent large events (Chapter 1, Abeyta and Paola, 2014). These mass flow events alter dramatically the local shoreline geometry by changing the gradient of sediment flux along the delta (Chapter 3), seen here in the form of land loss in inactive portions of the delta and deep, migrating knick-points. The features formed as a result of these complex mass flows include channel and levee structures in the offshore (Fig.2-11)

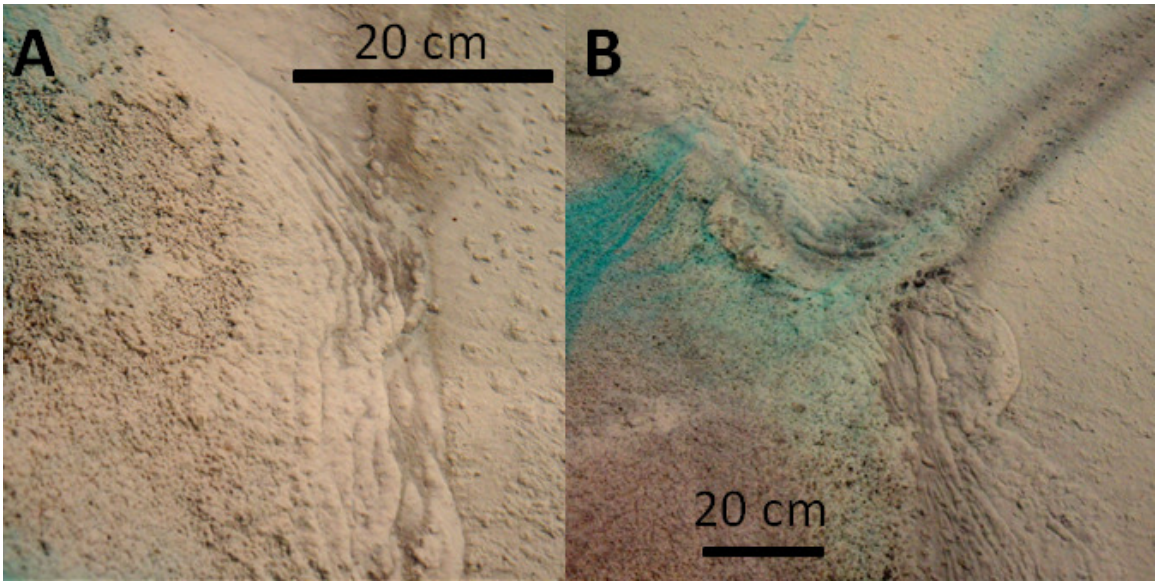

Figure 2-11 A. Failure ridges from mass failure events on the clinoform foreset, these features are only observed in the cohesive expeirments. B. Channel and levee structure from mass failure events in the offshore in a cohesive system.

Large scale morphology

Shoreline complexity

Shorelines in the cohesive deltas in general had more complex shorelines with lower measured area-deficit ratios than in the non-cohesive deltas. The reason for this is the long channel occupancy times and rapid shifting of the channel in the cohesive deltas, which promote the development of strongly expressed sub-deltaic lobes. However, the purely cohesive system, the floc delta, had the simplest shorelines with area-deficit ratios close to 1. The floc delta acted and behaved more like a non-cohesive system, similar to previous delta experiments and the non-cohesive experiment in this study. The only deviation from a ratio of unity was due to a transient lobe-building event. We speculate that over time, this ratio would approach 1 as the floc system tended to have channels that were broad and shifted across the delta surface. The flocculated clay sediment behaved more like the sandy, non-cohesive systems, consistent with observations in previous experimental work (Schieber et al., 2007; Schieber and Southard, 2009; Schieber and Yawar, 2009).

In fluvial systems, the measured area-deficit ratios varied a great deal during the initial building phase of the experiment. Once the delta was established, shoreline area-deficit measurements varied around a mean ratio of 0.95 for non-cohesive systems and 0.87 for cohesive systems (Fig. 2-12). The increased shoreline complexity seen in fluvial systems can be attributed to two factors: the long channel occupancy times and consequent lobe development, and mass failure events that lead to episodic, localized land loss.

Tides had different influences on shoreline complexity for the two sediment types. In the non-cohesive deltas, area-deficit ratios approached 1, suggesting a smoothing of the shoreline. The tide washing over the delta combined with the lower thresholds for sediment transport allowed the tides to rework the shoreline. The opposite was the case for the cohesive systems, where tides created more complex shorelines with lower area-deficit ratios. Tides in the experiment resulted in mass failure events which took bites off of the topset through time. While this may have been partly a result of the sediment mix used due to the more pronounced failures (Chapter 1), it is important to note that the tides increased the channel occupancy time greatly in the cohesive system, which promotes the formation of sub-deltaic lobes that in turn increase area-deficit ratios and shoreline complexity.

Waves dramatically reworked the shorelines of both systems over extremely short time scales compared to the overall experiment, on the order of one hour. The shorelines produced in the wave settings tended to produce high area-deficit ratios, which indicate shoreline simplicity (Fig. 2-12). In the non-cohesive delta, there was a slight reduction in area-deficit ratios due to constant beach reworking of the shoreline. In the cohesive system, shoreline simplicity initially increased, where the shoreline is smoothed out by the waves (Fig. 2-12). However, the presence of high amplitude waves proved to be destructive, removing more sediment to the offshore than was being reworked to build beach deposits (Fig. 2-12). This suggests that the strength of waves may be a limiting factor for the preservation of deltaic deposits.

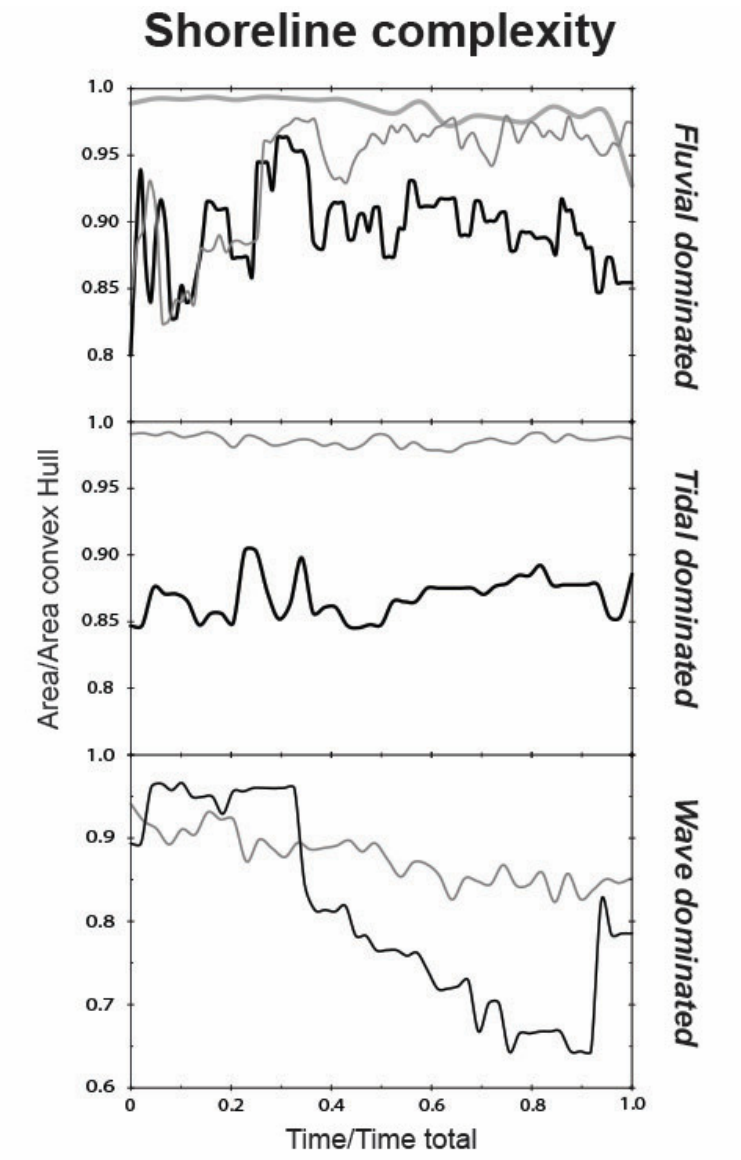

Figure 2-12 Shoreline complexity over time under different forcings. Shoreline complexity is defined as the ratio of the area of the object over the area of the convex hull.

Slopes

The slopes on the topset and flood plain for both sediment types again tend to be lower than those for traditional silica-sand mixes because of the reduced density of the walnut sand (Table 2-3). The cohesive mix had steeper topset slopes than its non-cohesive counterpart. The difference between the transport slope and the topset slopes in

non-cohesive systems tended to be comparable, with the topset being slightly steeper than the channel slope (Table 2-3). In the cohesive system, the differences between the slopes in the channel and the topset slopes were much greater, with the topset slope almost double the channel slope (Table 2-3). The strong difference between the topset and channel slope combined with the increased critical shear stress of the system causes the channel to prefer to occupy pre-existing channels during avulsions rather than form new channel positions: carving a newer channel would, in a sense, require a higher activation energy (Fig. 2-6, Miyamoto et al., 2005).

DISCUSSION

We often ascribe the many shapes and features observed in deltaic deposits to the influence of external forces (relative fluvial, tidal, and wave effects) acting on the system. However, the experiments shown here illustrate how much of the large-scale morphology and behavior are determined at the grain scale. While experiments are much simpler than natural systems, the results presented here are largely the result of a basic aspect of cohesion that is generic and independent of scale: it sets a threshold that makes deposited sediment harder to re-entrain than it would otherwise be. This effect, which leads to the morphologic and behavioral effects detailed above, indicates that cohesion sets an important geomorphic threshold for determining the morphological deltaic features. Thus, we return to Victor Hugo's view of the world, asking to what extent the features we observe are determined at the grain scale and find that the grain scale appears to be just as important for setting morphological features as the external influences acting on the system.

While there has not been a comprehensive study looking at the role of cohesion on setting geomorphic features of deltas in the field, the experiments described here highlight some of the trends we expect to find, starting with increases in shoreline complexity as measured by the area-deficit ratio defined above. This represents an easily

measureable parameter that can be applied to modern deltas, and even to ancient examples where they are well imaged seismically (Posamentier et al., 1992; Deptuck et al., 2012).

Our findings also have implications for the ways which we understand, manage and restore natural deltas. For example, the Mississippi delta, some researchers have suggested creating channel diversions to combat significant land loss (Nittrouer et al., 2012). In order for such methods to yield promising results, one must consider how the role of cohesion may influence factors such as channel dynamics, channel morphology, bar deposition and shoreline complexity.

CONCLUSIONS

The experiments described in this paper show that there are significant differences between the morphodynamics of cohesive and non-cohesive deltas under otherwise similar influences of rivers, waves, and tides; specifically:

1) Cohesive deltas produce channels with lower width to depth ratios that have better defined thalweg and floodplain features than non-cohesive deltas.
2) The transport slopes are comparable for both sediment types and are set by the water and sediment inputs. Waves effectively increase the transport slope as a result of adjusting to the reworking and removal of sediment at the shoreline. There is an apparent difference between the topset slope and the channel slope in cohesive systems that is not observed in non-cohesive systems.
3) Cohesive systems produce more sinuous channels, but tides increase channel sinuosity for both sediment types.
4) Channels persist over significantly longer time scales in cohesive systems and tides stabilize channels for both sediment types, significantly reducing channel mobility. Waves also increase channel stability but to a lesser extent than do tides.

5) Non-cohesive channels avulse by sweeping across the topset while cohesive channels change position abruptly and typically reoccupy previously existing channels.
6) Cohesive systems produce and preserve bars at a higher frequency than non-cohesive systems and the bars produced are smaller, with higher aspect ratios. The presence of waves or tides hinders the formation and preservation of bar deposits for both sediment types.
7) Cohesive deltas have complex offshore dynamics associated with highly variable failure size that result in land loss in inactive portions of the delta and can form deep, migrating knick points. These migrating knick points can increase the channel occupancy significantly, promoting the formation of sub-deltaic lobes and influencing overall planform morphology.
8) The shorelines produced by cohesive systems tend to be more complex, as measured by the area-deficit ratio (area of delta top/area of convex hull). However purely cohesive floc deltas produced the simplest shorelines and generally behaved more like a non-cohesive system.

REFERENCES

Abeyta, A. and **Paola, C.**, 2014, The transport dynamics of mass failures along weakly cohesive clinoform forests. *Sedimentology*, 62, p. 303-313.

Bain, R., 2014, A Comparison of the Planforms of Meandering Tidal and Fluvial Channels on the Ganges-Brahmaputra-Jamuna Delta, Bangladesh. (Master's Thesis), *University of Minnesota.*

Deptuck, M.E., Mohrig, D., Van Hoorn, B., and **Wynn, R.B.**, 2012, Application of the principles of seismic geomorphology to the continental slope and base of slope systems:

Case studies from sea floor and near shore analogs. *Society of Sedimentary geology*, p. 145-161.

Edmonds, D. and **Slingerland, R.**, 2009, Significant effect of sediment cohesion on delta morphology. *Nature Geoscience*. 3, p. 105-109.

Edmonds, D. A., Paola, C., Hoyal, D. C., and **Sheets, B. A.**, 2011, Quantitative metrics that describe river deltas and their channel networks. *Journal of Geophysical Research: Earth Surface,* 116, 2003-2012.

Fagherazzi, S., Gabet, E. J., and **Furbish, D. J.**, 2004, The effect of bidirectional flow on tidal channel planforms. *Earth Surface Processes and Landforms*, 29, p. 295-309.

Galloway, W., 1975, Process Framework for Describing the Morphology and Stratigraphic Evolution of Deltaic Depositional Systems. *Deltas Models for Exploration*, p. 87-98.

Gastaldo, R. A., Allent, G., and **Huci, A. Y.**, 2009, The tidal character of fluvial sediments of the modern Mahakam River delta, Kalimantan, Indonesia. *Tidal Signatures in Modern and Ancient Sediments (Special Publication 24 of the IAS)*, 28, 171.

Hoyal, D. C. J. D., and **Sheets, B. A.**, 2009, Morphodynamic evolution of experimental cohesive deltas. *Journal of Geophysical Research*, Earth Surface, 114(F2).

Hugo, V., 1862, *Les Miserables.*

Keshavarzi, A. and **Habbi, L.**, 2005, Optimizing water intake angle by flow separation analysis. *Irrigation Drainage*, 54, p. 543-552.

Larsen, L., Harvey, J.W, Noe, G.B., and **Crimaldi, J.P**., 2009, Predicting organic floc transport dynamics in shallow aquatic ecosystems: Insights from the field, the laboratory, and numerical modeling. *Water resources Research*, 42, W01411.

Levin, D. R., 1995, Occupation of a relict distributary system by a new tidal inlet, Quatre Bayou Pass, Louisiana. *Tidal Signatures in Modern and Ancient Sediments. Special Publication 24 of the IAS*, 9, 71.

Martin, J., Sheets, B., Paola, C., and **Hoyal, D.**, 2009-A, Influence of steady base-level rise on channel mobility, shoreline migration, and scaling properties of a cohesive experimental delta. *Journal of Geophysical Research*, 144, F3, F03017.

Martin, J., Paola, C., Abreu, V, Neal, J., and **Sheets, B.**, 2009-B, Sequence stratigraphy of experimental strata under known conditions of differential subsidence and variable base level. *AAPG Bulletin*, 93, p. 503-533.

Miyamoto, H., Baker, V. R., and **Lorenz, R. D.**, 2005, Entropy and the Shaping of the Landscape by Water, *Springer Berlin Heidelberg*, Ch. 11, p. 135-146.

Nittrouer, J. A., Best, J. L., Brantley, C., Cash, R. W., Czapiga, M., Kumar, P., and **Parker, G.**, (2012), Mitigating land loss in coastal Louisiana by controlled diversion of Mississippi River sand, *Nature Geoscience*, 5, p. 534-537.

Orton, G. and **Reading, H.**, 1993, Variability of deltaic processes in terms of sediment supply, with particular emphasis on grain size. *Sedimentology*, 40, p. 475-512.

Paola, C., Mullin, J., Ellis, C., Mohrig, D., Swenson, J.B., Parker, G., Hickson, T., Heller, P., Pratson, L., Syvitski, J., Sheets, B., and **Strong, N.**, 2001, Experimental stratigraphy. *GSA Today*, 11, p. 4-9.

Parker, H., 1996, River meandering as self-organization process. *Science*, 271, pp. 1710.

Passalacqua, P., Lanzoni, S., Paola, C., and **Rinaldo, A.**, 2013, Geomorphic signatures of deltaic processes and vegetation: The Ganges-Brahmaputra-Jamuna case study. *Journal of Geophysical Research: Earth Surface*, 118, p. 1838-1849.

Pirmez, C., 1998, Clinoform development by advection-diffusion of suspended sediment: Modeling and comparison to natural systems. *Journal of Geophysical Research*, 103, p. 24,141–24,175.

Posamentier, H.W., Allen, G.P., and **James, D P.**, 1992, High resolution sequence stratigraphy- the east Coulee Delta, Alberta. *Journal of Sedimentary Research*, 62, no. 2.

Schieber, J., Southard, J., and **Theison, K.**, 2007, Accretion of Mudstone Beds from Migrating Floccule Ripples. *Science*, 318, p. 1760-1763.

Schieber, J. and **Southard, J.,** 2009-a, Bedload transport of mud by floccule ripples – Direct observations of ripple migration processes and their implications. *Geology*, 37, p. 483-486.

Schieber, J. and **Yawar, Z.,** (2009-b) A New Twist on Mud Deposition – Mud Ripples in Experiment and Rock Record. The Sedimentary Record: Vol. 7, no. 2, pp. 4-8.

Smart, J. S., and **Moruzzi, V. L.**, 1971, Quantitative properties of delta channel networks. IBM Thomas J Watson Research Center, Yorkston Heights, NY, No. Tr-3.

Chapter 3

3

SINK TO SOURCE: THE EFFECT OF OFFSHORE DYNAMICS ON UPSTREAM PROCESSES*

*Submitted as Abeyta, A., Foreman, B.Z., Swenson, J., Paola, C., and Mohr, J. *Sink to Source: The effect of offshore dynamics on upstream processes* to Basin Research.

SUMMARY

When we model fluvial sedimentation and the resultant alluvial stratigraphy, we typically focus on the effects of local parameters (e.g., sediment flux, water discharge, grain size) and the effects of regional changes in boundary conditions applied in the source region (i.e., climate, tectonics) and the shoreline (i.e., sea level). In recent years this viewpoint has been codified into the 'source-to-sink' paradigm, wherein major shifts in sediment flux, grain-size fining trends, channel-stacking patterns, floodplain deposition, and larger stratigraphic systems tracts are interpreted in terms of tectonic and climatic signals originating in the hinterland that propagate downstream, and eustatic fluctuation, which sets the position of the shoreline and dictates the generation of accommodation. Within this paradigm, eustasy represents the sole means by which downstream processes may affect terrestrial depositional systems. Here we provide three experimental cases in which coastal rivers are strongly influenced by offshore and slope transport systems via the clinoform geometries of typical of prograding sedimentary bodies and support a 'sink-to-source' view of fluvial-deltaic systems. The experimental series illustrates the effects of (1) submarine delta front failure events, (2) deformable substrates within prodelta and offshore settings, and (3) submarine hyperpycnal flows. These submarine processes affect

knickpoint generation, river channel occupancy times, rates of shoreline movement, and the location of dominant sediment accumulation. Ramifications for coastal plain and deltaic stratigraphic patterns include changes in the hierarchy of scour surfaces, fluvial sand-body geometries, reconstruction of sea-level variability, and large-scale stratal geometries, all of which are linked to the identification and interpretation of sequences and systems tracts.

INTRODUCTION

The rich textures, fabrics, and features of the Earth's skin are shaped by sediment mass fluxes across the surface. Sediment is eroded from upland mountains and hillsides, routed through terrestrial and marine basins, and eventually deposited to form the stratigraphic record. The stratigraphic record displays organization and patterns on a range of scales related to local transport conditions (Paola and Borgman, 1991; Bridge, 1997), landscape topography (Bown & Kraus, 1987; Kraus, 1997) autogenic geomorphic processes (Hajek et al., 2010; 2012), and basin geometry (Straub et al., 2009; Straub and Pyles, 2012) among other factors (Allen, 2008). To understand this system, we might ask questions such as: where does this sediment come from and how did it get here? More importantly, what controls sedimentation on large space and time scales? The natural response to many of these questions is to look upstream – to where the sediment and water come from – for the answers and, by extension, to determine how changes within the source region affect the resulting deposit in the sink. This predisposition has led to the development of a conceptual framework known as *source-to-sink*, in which major shifts in sediment flux, grain-size fining trends, channel stacking patterns, floodplain deposition, and larger stratigraphic systems tracts are mainly interpreted in terms of tectonic and climatic signals originating in the hinterland (Allen, 2008; Duller et al., 2010; Whittaker et al., 2010; Foreman et al., 2012; Foreman, 2014; Covault et al., 2010). Yet the flow of information in landscapes is bidirectional, and one line of theoretical analysis suggests that it tends to be from downstream toward upstream in depositional systems (Voller et al., 2012).

Chapter 3

The source-to-sink paradigm places linked transport systems in a mass balance framework, where there are sediment inputs and sediment is sequestered in sinks. Erosion-dominated landscapes are viewed as the ultimate sediment source with signals propagating downstream, partially recorded within terrestrial basins acting as sinks controlled by subsidence, and ultimately sequestered within marine basins (Allen, 2008). Subsidence and accommodation, either tectonically or eustatically generated, dictate the size (capacity) of the sink. The ability of tectonic and climatic changes in the source area to affect deposition within terrestrial basins is well established from field, experimental, and numerical model studies (Hickson et al., 2005; Kim et al., 2006; Kubo et al., 2005; Armitage et al., 2011). Moreover, there are definitive stratigraphic impacts due to associated shifts in sediment supply, grain size, basin slope, and subsidence geometry. These include downstream changes in (1) grain size, (2) the character of lithofacies and internal architecture of fluvial deposits, (3) paleo-flow depths, (4) channel-stacking density, (5) basin-scale soil development, and (6) widespread lacustrine deposition (Leeder, 1978; Allen, 1978; Bridge and Leeder, 1979; Bown & Kraus, 1987; Paola et al., 1992; Heller and Paola, 1992; Heller and Paola, 1996; Carroll and Bohacs, 1999; Kraus, 1997; Foreman et al., 2012; Foreman, 2014). Typically the stratigraphic response to tectonic and climatic forcing in the source is thought to be most pronounced in proximal locations and attenuated in distal, coastal areas; however, there are examples of significant coastal and marine responses to tectonic and climatic perturbations in their associated upland areas (Kostic et al., 2002; Porebski and Steel, 2003; Brown et al., 2004). Here we focus predominantly on coastal river and shoreline systems, which are typically part of the sink in the source-to-sink context.

When we consider factors controlling the local mass-balance condition of coastal rivers (sediment and water supply), relative sea level plays a major downstream control (e.g., Penck and Briclmer. 1909; Fisk, 1944; Sloss, 1962; Schumm, 1993; Blum and Törnqvist, 2000 and references therein). Because sea level sets the downstream boundary condition for coastal rivers, it provides an obvious exception to the source-to-sink focus on how changes within the source are propagated and recorded downstream toward the

sink. The combination of sea level as a downstream control with source-side (upstream) controls led Holbrook et al. 2006 to propose the idea of "buffers and buttresses", in which the downstream controls are thought of as buttresses that inhibit the onward flow of sediment. A number of recent studies have considered how changes propagate upstream from the shoreline in coastal river systems (Swenson, 2005; Hoyal and Sheets, 2009; Chatanantavet et al., 2012; Lamb et al., 2012), Here we consider an extension of this idea by asking how changes within the sink affect the upstream behavior of a depositional system.

We illustrate 'sink to source' signal propagation via three examples of how conditions well offshore of the shoreline can control mass balance within and behavior of coastal plain rivers and shorelines and, by extension, influence the resultant stratigraphy. These extend the well-known action of sea level as a downstream control by including results stemming from the observation that coastal rivers are generally coupled to offshore and slope transport systems via the clinoform geometries of typical of prograding sedimentary bodies. The clinoform is a linked system, and as a result of this coupling, changes within the depositional system beyond the shoreline can profoundly influence upstream behavior. We provide three experimental studies to illustrate this point. The experiments are not aimed at explicitly reproducing a specific location or sedimentary system but rather illustrate the effects on the fluvial system of three types of offshore dynamics (i.e., sediment gravity flows, cohesive mass failures, and fault-associated delta front failures triggered by differential loading of a deformable substrate) All of these are conditions known to exist in field-scale coastal systems(Kostic et al., 2002;, Madof et al., 2004, Webster et al., 2013). Our hope is that future, field-based work will elucidate the degree to which offshore processes affect coastal systems. Hence, our experiments should be viewed as examples for how coastal systems may respond if offshore dynamics are the dominant control on onshore behavior. Importantly, the processes explored within affect onshore dynamics and stratigraphy independent of eustatic variability, but have substantial repercussions for our identification and interpretation of parasequence generation, sequence boundaries, and systems tracts.

Chapter 3

CONCEPTUAL FRAMEWORK

To illustrate the concept of offshore events influencing the overall mass balance of a costal river, consider a simple one-dimensional prograding fluvial deltaic system. The system comprises a topset, a foreset, and a bottomset, which are linked at the shoreline and the foreset toe (Figure 3-1). Under steady conditions, this linked depositional system progrades as an approximately self-similar waveform, i.e. a clinoform. Over the length of the system, deposition is associated with downstream decrease in sediment flux to balance mass. The first critical point in this linked system is the shoreline, where nearshore processes, e.g. longshore drift, can reduce the sediment supplied to the delta foreset, thereby reducing the progradation rate. A second critical point in the overall mass balance—and the point we emphasize here—is the delta toe, which acts as a *choke point*, which we define as a persistent local minimum in the sediment flux. If the flux is zero at the toe then all the supplied sediment must be deposited upstream of this point, thereby maximizing the progradation rate. It follows then that the state of deposition upstream of the toe must be controlled by transport conditions at the toe.

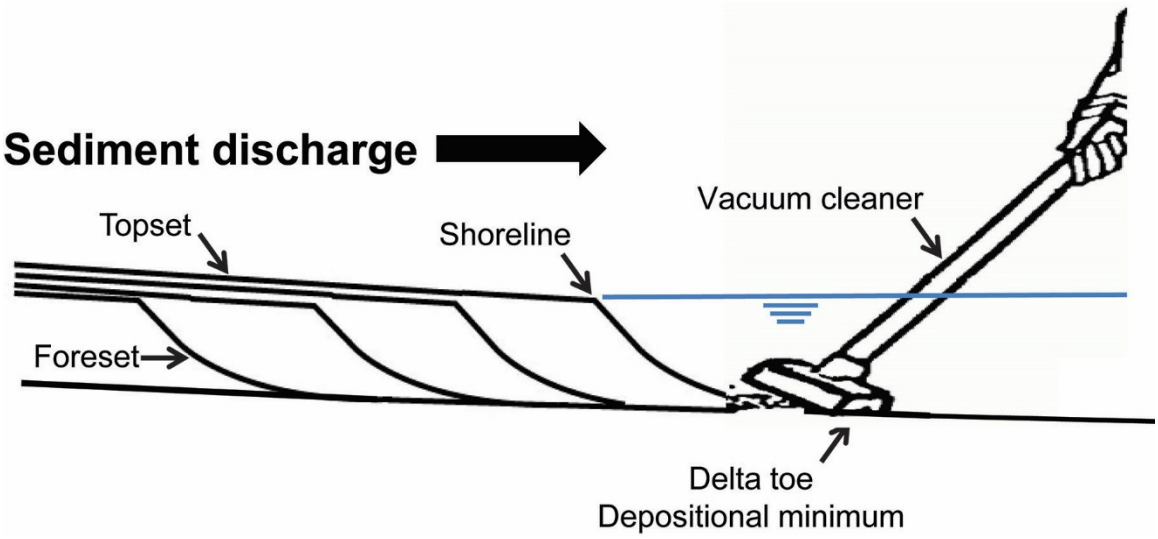

Figure 3-1 An example of a simple one-dimensional prograding fluvial deltaic system. Along the delta, deposition is associated with the change in sediment flux, where the delta toe is a local sediment minimum. In this paper, we explore how changes in sedimentation rates at the local depositional minimum are reflected.

Consider a vacuum cleaner

One way to see how the delta toes exerts control is to imagine a vacuum cleaner attached to the delta toe to remove sediment (Fig. 3-1). How would changing the removal rate affect the system upstream? When the vacuum is turned on, removing sediment at the toeset, the upstream mass balance has to adjust to replace the lost sediment. In the context of a mass balance framework, we are changing the strength of the sink and in order to maintain mass balance, the gradient of sediment flux must change upstream to accommodate that. This concept can be quantified using the one-dimensional Exner equation, where η is the bed elevation, ε is the grain packing density, q_s is the sediment discharge:

$$\frac{\partial \eta}{\partial t} = \frac{-1}{\varepsilon_o}\frac{\partial q_s}{\partial x} \qquad 3\text{-}1a$$

Integrating Eq. 3-1a from the initial point of net deposition ($x = 0$) to the toe ($x = x_{min}$), where there is an imposed minimum in the flux, we see (3-1b) that the mean rate of deposition between x_0 and x_{min} is just the difference between the source flux (flux maximum) and the flux at the toe (the flux minimum).

$$\bar{r} \cdot x_{min} = \int_0^{x_{min}} r dx = q_{so} - q_{min} \qquad 3\text{-}1b$$

Thus, any change in the sediment flux at the downstream end changes the flux difference and thus the average deposition rate between 0 and x_{min}. In that sense, downstream conditions (here the condition at x_{min}) are just as important as upstream conditions (here, the source flux at x_0) in controlling the mass balance regime between x_0 and x_{min}.

If the sink at the downstream end is strong enough i.e. if some process can extract sediment at the rate supplied by the source so that $q_{min} \rightarrow q_{so}$, then the system changes from net aggradation to net bypass, or even erosion if $q_{min} > q_{s0}$. We define the system as *choked* for $qs_{min} < qs_0$ and *unchoked* for $q_{min} \geq q_{s0}$. Morphodynamically, this induced change in sink strength is similar in its effects on the fluvial system to a fall in relative

sea level (e.g., Blum and Törnqvist, 2000). The resulting stratal architecture could easily be ascribed to a fall in relative sea level, or other external factors such as an increase in the ratio of water to sediment discharge. Although sequence stratigraphy has long since outgrown its initial narrow focus on sea level changes, the association of relative sea-level fall, fluvial bypass, and offshore accumulation of coarse sediment is common and often reasonable, and so continues to influence the interpretation of the stratigraphic record (e.g, Catuneanu, 2006).

Now it may seem silly to consider a vacuum cleaner at the delta toe, but there are a variety of natural scenarios that can produce the same effect in terms of changing the strength of the sink. Mechanisms that affect the sediment transport along the foreset include slope-driven mass failures, hyperpycnal currents, waves, and external currents. Any of these, singly or in combination, could influence the transport rate in the foreset region and thus the overall mass balance upstream on the clinoform. In the next sections we illustrate three such mechanisms: (1) enhancing transport on the foreset via hyperpycnal turbidity currents, (2) mass failure on the delta foreset, and (3) local subsidence due to substrate deformation. In the first case, the experiment was designed to study changes in the fluvial system as a result of slight changes in the offshore mass balance very close to the transition between the choked and unchoked condition in Eq. 3-1.

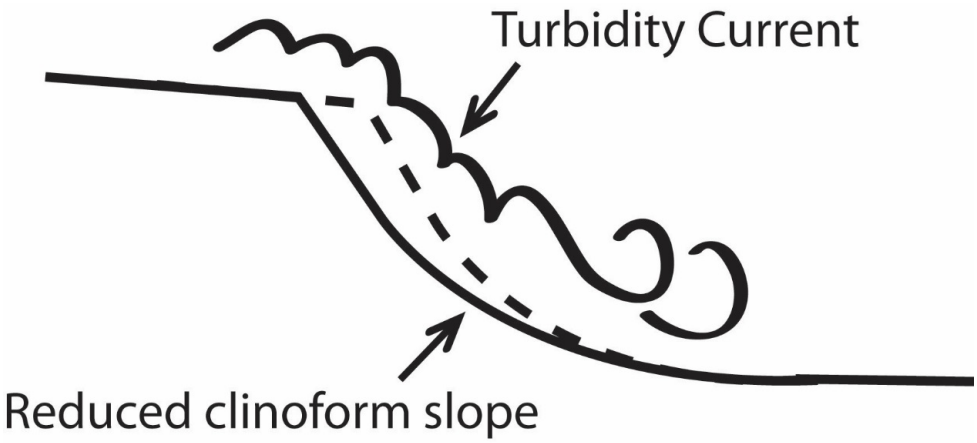

Figure 3-2 Previous experimental work by Kostic and Parker, 2002 shows that hyperpycnal flows can reduce the slope of the delta foreset Case study 1: Hyperpycnal flows

Chapter 3

CASE STUDY 1: HYPERPYCNAL TURBIDITY CURRENTS

The toe of a mass-flow dominated clinoform foreset functions as an imposed minimum in sediment flux (i.e. as a choke point) as long as the clinoform progrades over topography with a slope below the failure slope of the foreset. In that case, a simple mechanism for clearing the choke point is to change the relationship between the foreset slope and the slope of the topography it advances across. The slope of a clinoform foreset can be reduced by overpassing hyperpycnal turbidity currents (Kostic et al., 2002; Fig. 3-2). If a system experiences a rise in turbidity current activity on the foreset as a result of increased sediment concentration or from the generation of wave-supported gravity flows ('fluid muds'; Kineke et al., 1996; Friedrichs and Scully, 2007), then this should result in a reduction of the foreset slope. If the foreset slope were reduced to a slope less than that of the underlying shelf surface, sediment would no longer accumulate at the base of the foreset and the choke condition at the delta toe would be removed, changing the transport path from a choked to an unchoked condition. By the reasoning presented above, the fluvial system should then switch to bypass mode and the sediment formerly trapped in the foreset transferred into deeper-water environments.

Methodology

To study scenarios close to the transition from fluvial aggradation to fluvial bypass, we conducted four experiments in a narrow, glass wall flume 2 cm wide by 4 m long, with a constant base level of 17 cm. In each experiment, we supplied a constant discharge of water and quartz sand (D_{50} = 110 μm) to create a simple two-dimensional deltaic system with a foreset slope at the angle of repose. The delta prograded over an initial horizontal surface that led to an inclined ramp (Fig. 3-3) set to an angle (26˚) slightly less than the angle of repose. Once the toe reached the ramp, we either changed nothing, allowing the clinoform to prograde continuously down the ramp, or we added a fixed concentration of silica silt (D_{50} = 40 μm) to the sediment and water supply. The silt increased the density of the sand-water mixture and created a plunging hyperpycnal turbidity current on the foreset. The amount of silt sequestered in the fluvial system was volumetrically insignificant and the silt was transported mainly in suspension over the

length of the experiment. The silt concentration was constant once it was introduced, but we supplied four different concentrations to change the strength of the hyperpycnal flow. Using photographs, we measured the evolution of the long profile of the deltaic system in time and space. From this analysis, we computed the fluvial aggradation rate as a function of position and reconstructed the stratigraphic evolution of each experiment.

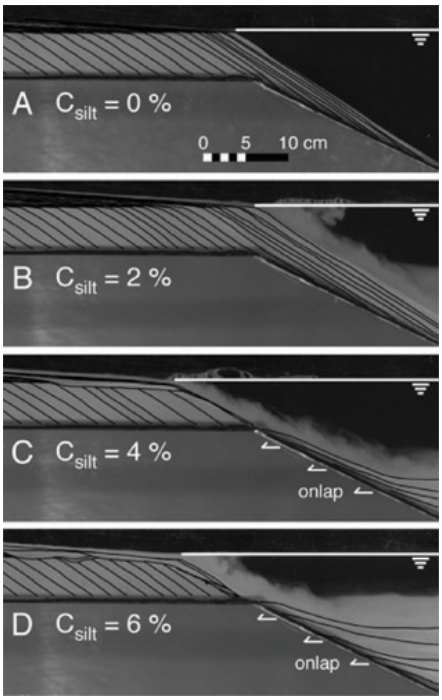

Figure 3-3 Reconstructed experimental strata (timeline spacing is two minutes). (A) *Csilt* = 0%. (B) *Csilt* = 2%; insufficient reduction in foreset slope to 'un-choke' system. (C) *Csilt* = 4%; (D) *Csilt* = 6%. In both (C) and (D), reduction in foreset slope 'un-choked' system, resulting in sediment transfer to the base of slope. Also, local reworking ('cut and fill' cycles) of the fluvial system caused by upstream propagation of autogenic, cm-scale knickpoints.

Observations

In experiments without any hyperpycnal flows, the delta continued to prograde across the ramp, albeit at a decreasing rate due to the increasing foreset length (Fig. 3-3). This was also true for the lowest concentration of added silt, which was not sufficient to reduce the foreset slope below that of the imposed ramp. Thus in these two cases, the transition from a horizontal to a sloping substrate surface did not affect the aggradational state of the fluvial system. But increasing the silt concentration to 4% or greater caused a

dramatic, qualitative change in the behavior of the entire system: the foreset slope was reduced below the slope of the ramp, at which point the clinoform toe no longer functioned as a choke point and the choke condition was removed. The result of this change was to halt clinoform progradation, and the fluvial system immediately switched from aggradation to bypass and erosion mode. The transport system bypassed the entire sediment supply and that sediment accumulated instead at the base of the ramp in a subaqueous fan that onlapped the sloping ramp (Figs. 3-3 and 3-4). The abrupt transition away from a state of net aggradation in the fluvial system resulted in erosion in the fluvial system. Hence the combination of an underlying topographic slope in deep water well beyond the shoreline with fine suspended sediment to produce a hyperpycnal turbidity current led to an abrupt change from aggradation to bypass in the fluvial system. It is also noteworthy that this change from fluvial aggradation to bypass was caused by an *increase* in the overall sediment supply to the system – albeit involving finer sediment.

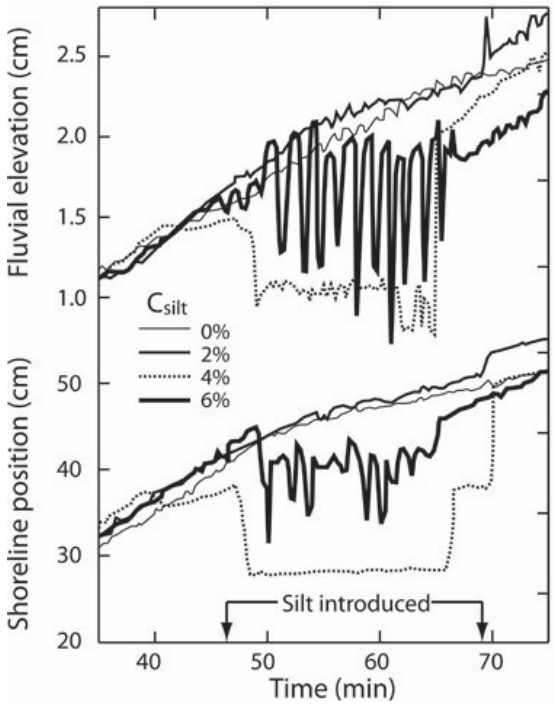

Figure 3-4 Shoreline position and fluvial elevation (0.2 m downstream from sediment source) for experiments shown in Figure 3-3. Shoreline progradation and fluvial aggradation continue throughout the entire experiment with low concentration (*Csilt* = 0% and 2%) turbidity currents. In contrast, shoreline progradation and fluvial aggradation are interrupted, i.e. system is 'unchoked', in experiments with higher concentration (*Csilt* = 4% and 6%) turbidity currents.

CASE STUDY 2: MASS FAILURES

Methodology

Abeyta and Paola (2014) developed a sediment mix (a 1 to 1 ratio mix by volume of walnut sand and kaolinite clay) to study the influence of discharge on the size and frequency of mass failure events. In a series of experiments with a narrow (1D) clinoforms, a major effect of adding cohesive sediment was to alter foreset mass-flow dynamics away from the fairly regular small avalanches characteristic of cohesionless grain flows to a range of mass failures including intermittent large events that substantially alter the local shoreline geometry. To understand how complex foreset dynamics such as mass failures affect overall deltaic behavior and morphology, we conducted experiments similar to those of Abeyta and Paola (2014) but in two dimensions in the Saint Anthony Falls Laboratory Delta Basin facilities. The Delta Basins are 5 m square and 0.6 m deep. The basins have a fixed horizontal floor, and base level is maintained by a computer-controlled weir and an attached siphon in the basin.

In the experiment in question here, we supplied constant water and sediment discharges of 0.1 L/s and 0.01 L/s respectively. Both were delivered from a point source in one corner of the basin. We maintained a constant base level of 160 mm, with no subsidence. An initial platform of sediment was built (1.5 m in radius and a height of 140mm) to expedite delta growth.

Observations

Evidence of mass failures on the delta front is apparent in the bathymetric profiles in time as well as landslide and failure ridges observed along the toe of the delta (Fig. 3-5). The landsliding events were most apparent in the inactive parts of the delta, possibly due to the fact that active deposition might make it difficult to distinguish land sliding events. . These events temporarily unlocked the choke point, moving sediment farther offshore. Because the volumes moved were relatively large, and the local sediment supply small (because they mainly affected inactive parts of the delta channel network), the failures temporarily changed the mass balance upstream of the landslide from net deposition to net erosion ($q_{min} > q_0$ in Eq. 3-1).

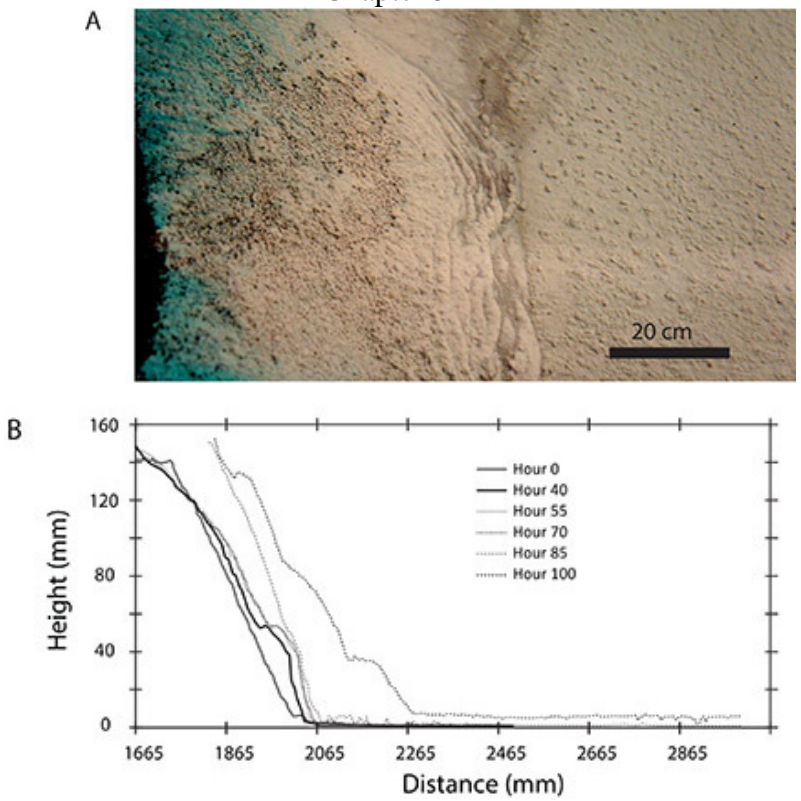

Figure 3-5 Image looking down at experimental deltaic foresets. Along the base of the foreset, are failure ridges due to mass wasting and slow creep. B) Additional evidence of mass movement along the clinoform foreset is seen in changes in bathymetric profiles in time.

The evidence for this is that the offshore landsliding events created migrating erosional knickpoints in the stream channels. The knickpoints formed at the channel mouth and migrated upstream, to respond to the change in sediment rate at the local minimum (Fig. 3-6). Migration of these knickpoints formed deep incised channels. These deeply incised channels made it difficult for water and sediment to breach the levees and avulse, leading to longer channel occupancy (inter-avulsion) time scales. To see if there was a characteristic length scale that marks the threshold of vertical elevation drop in the fluvial system to trigger a migrating knickpoint, we measured the initial "bite", i.e. the horizontal shoreline displacement, taken out of the fluvial system and multiplied it by the local slope to find the apparent elevation displacement associated with the landslide and consequent shoreline displacement. The estimated vertical drop in elevation is on the scale of the channel depth prior to the incision (Fig. 3-7).

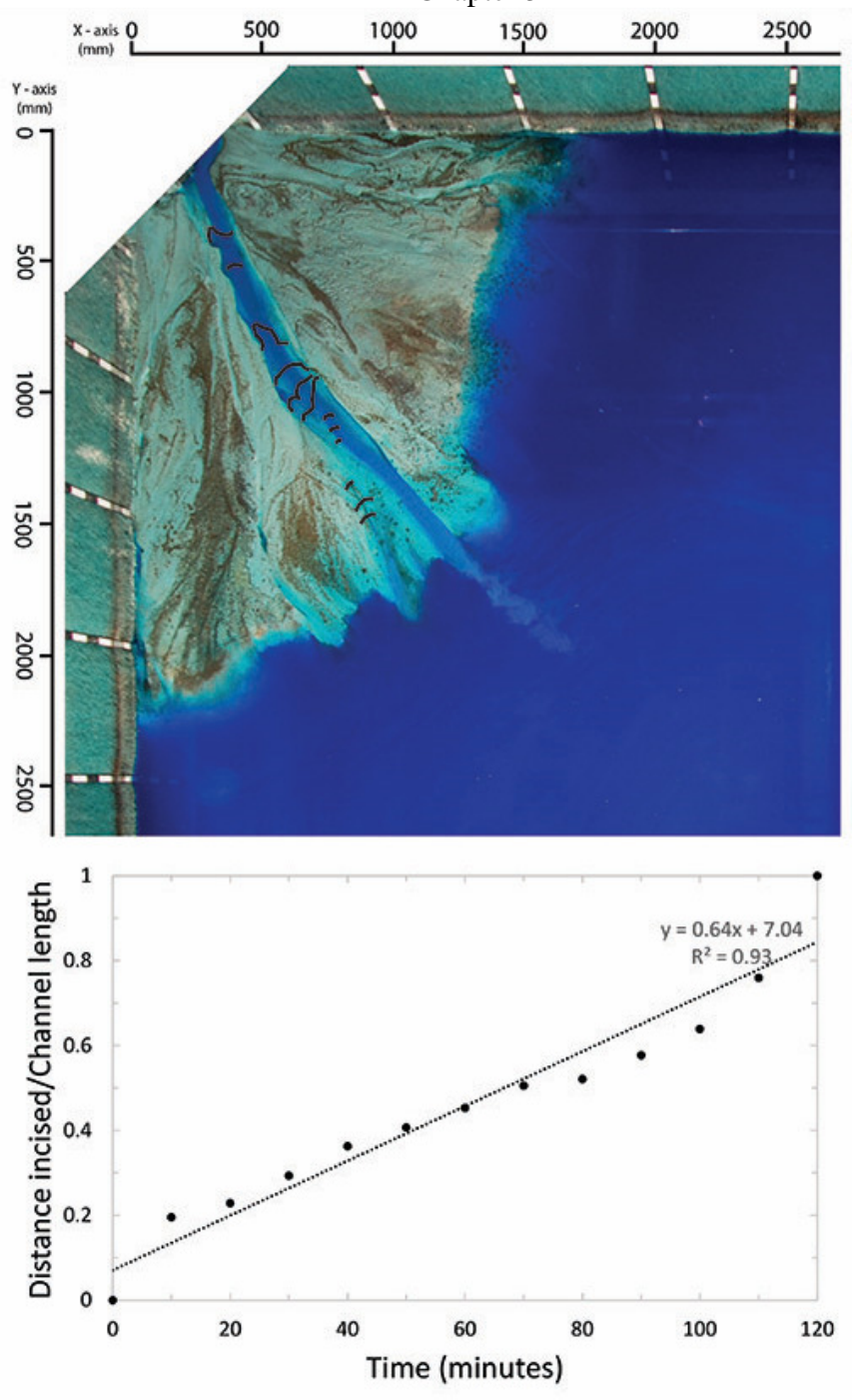

Figure 3-6 Mass failures resulted in the formation of channel knick-points which migrated upstream. The formation of these migrating knick points lead to deeply incised channels and increased the channel occupancy time. A) The location of the migrating knick points are marked in 10 minute intervals and B) migrated upstream at an almost constant rate, retreating at a rate of 1.7 cm per minute.

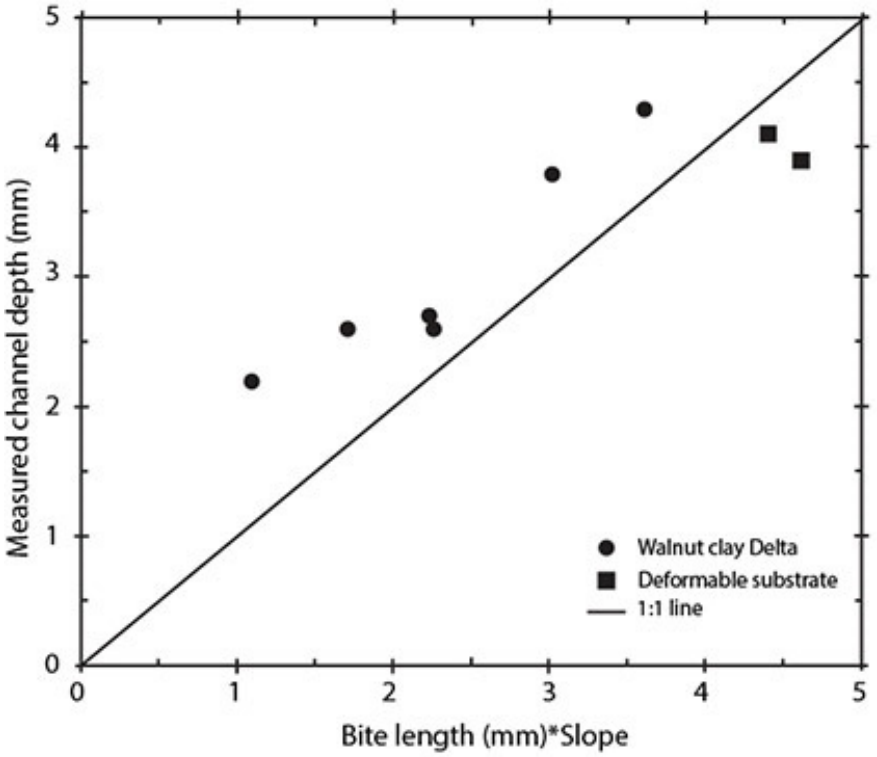

Figure 3-7 Initial bite length and the measured channel depth at the time of the incision. It suggests that the bite length is determined by the initial channel depth.

The result of temporarily removing the transport limit at the delta toe is a dramatic change in the behavior of the fluvial system and the resulting deposit on the topset. The landsliding events occurring in the offshore region also led to the extraction of sediment in inactive portions of the delta, contributing to a significant amount of shoreline retreat (Fig. 3-8). The combination of the land loss and the increased channel occupancy time from the knick-points led to a more complex and rugose coastline compared to otherwise similar experiments but without cohesive sediment, and thus lacking in this offshore dynamics (Fig. 3-9).

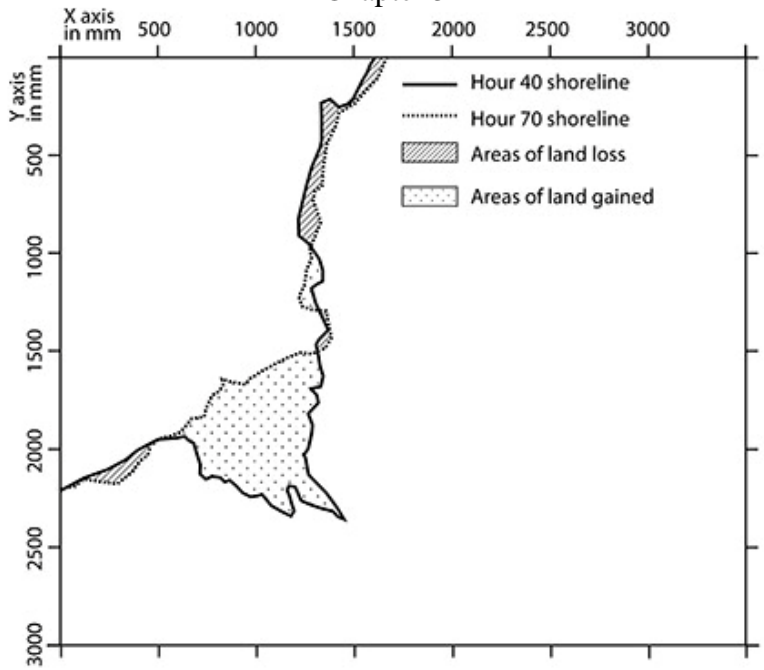

Figure 3-8 Shoreline position at hour 40 and hour 70. Shaded areas show regions where land was lost due to slow creep and mass wasting.

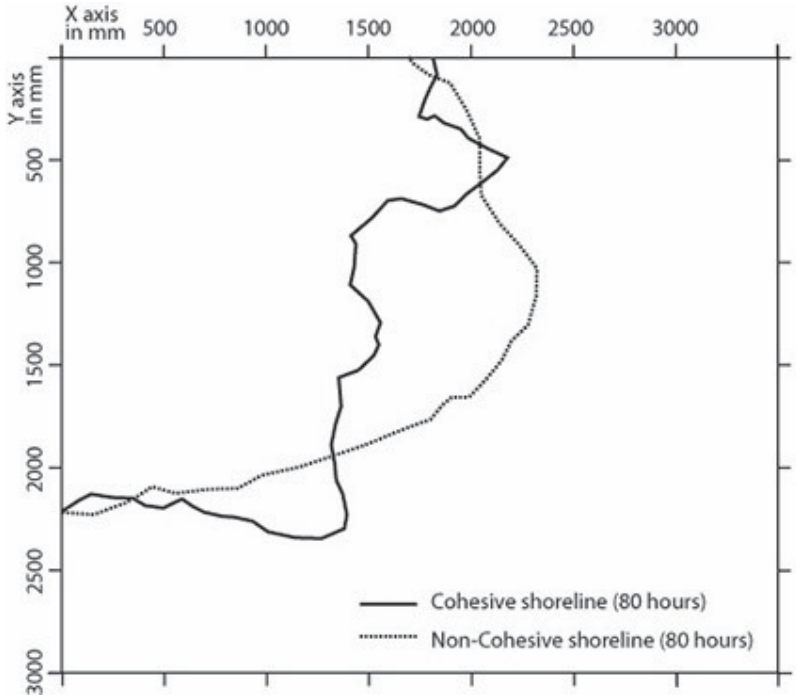

Figure 3-9 Comparison of two shorelines of a cohesive delta, which had complex offshore dynamics to a non-cohesive delta. Both deltas were built under exact same conditions with the only difference being the non-cohesive delta had no clay fraction. The shoreline of the cohesive delta shows a greater deal of complexity.

CASE STUDY 3: DEFORMABLE SUBSTRATES

A delta prograding over a mechanically weak layer, such as one made of halite or under-compacted muds results in a differential loading pattern over space and time that can deform the substrate (Madof et al., 2004) and substantially alter the sediment mass balance. Typically, this is thought to result in changes in the accommodation and sedimentation patterns in the distal end of the delta (Hudec et al., 2007). The sink-to-source framework presented here suggests that these distal influences of subsidence and accommodation could result in changes in the shoreline trajectory, channel behavior, and topset morphology. We designed an experiment to investigate the interactions between deltas and deformable substrates and their resultant effects on sediment mass balance.

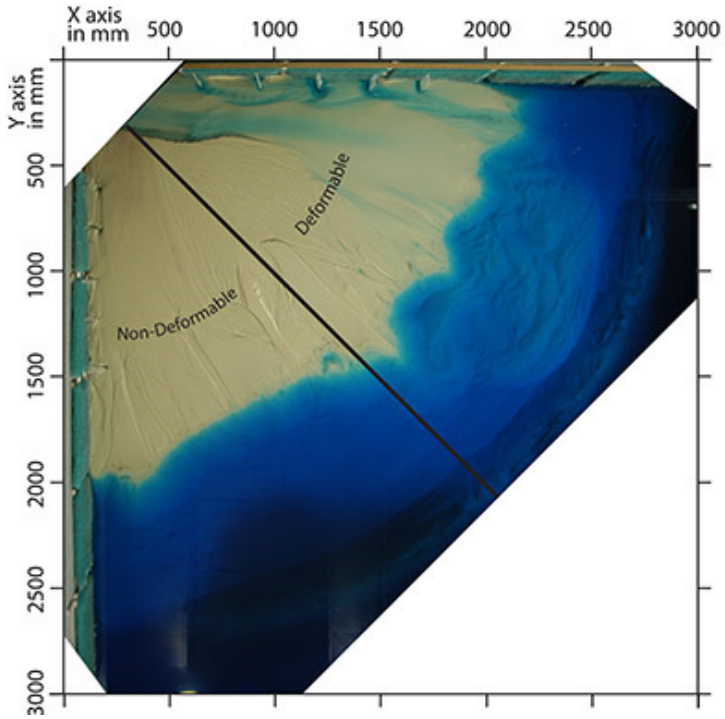

Figure 3-10 Image of 2D delta experiment with a deformable substrate. The basin was separated into two equal sections, one side containing a base layer of non-deformable sand and the other side containing a base layer made out of a deformable mix of kaolinite and clay. The deformable section of the experiment captured more of the channelized flow and contained more sediment deposited as seen in the offshore portion of the delta. Local faulting in the deformable substrate lead to rapid shoreline retreat.

Chapter 3

Methodology

The effect of substrate deformation on overall mass balance on the delta top is illustrated by a delta prograding over different substrate materials. This experiment was conducted in the delta basin as described in the previous section. A platform was constructed to provide a substrate for the delta to build over. The platform was divided into two equal-area sectors, one consisting of a 10 cm thick layer of deformable substrate and another consisting of a 10 cm thick non-deformable substrate (Fig. 3-10). The deformable substrate material in this case was a mixture of kaolinite clay and water with a 1:2 ratio by weight and a viscosity of 10 Pa·s. The non-deformable substrate consisted of coarse sand. In this experiment, we provided a constant supply of water 0.4 L/s and sediment (median grain size of 110 μm) 0.004 L/s. Sediment was delivered from a point source in the corner of the basin. We maintained a constant base level of 150mm.

Observations

Even though sediment was supplied to the entire clinoform with no directional preference, a substantially larger volume of sediment ended up on the deformable section of the delta (Fig. 3-10), similar to observations by Piliouras et al. (2014). The deformable side had increasing accommodation as a result of local subsidence of the substrate under sediment loading due to the delta prograding, causing the channel to remain on the deformable side of the delta for a greater fraction of time (Fig. 3-11). The subsidence also inhibited channel filling, which resulted in channels being able to maintain their position for longer time periods, creating elongated subaqueous lobes (Fig. 3-10). The substrate deformation led to longer channel occupancy (inter-avulsion) time scales in a similar manner to the offshore landslides discussed in the previous section. For our purposes, the main observation is that local subsidence of the deformable substrate sometimes occurred quickly enough to alter the shoreline geometry. These removed large volumes of deposit from the foreset quickly, again temporarily removing the choke condition, and altering the mass balance in the upstream fluvial system to one of net erosion. These changes produced upstream-migrating knickpoints, again similar to those discussed in the

previous case study (Fig. 3-10). However, these rapid erosional events of this experiment were caused by offshore collapse of the substrate and associated faulting rather than landsliding as in Case study 2. Estimating the minimal drop in vertical elevation as we did with Case study 2, we see that it scales closely to the channel depth prior to failure (Fig. 3-7). The fault motion, however, had a similar effect on the overall mass balance: removing sediment from the foreset and transferring it farther offshore, shortening and steepening the fluvial system, and switching it from net deposition to net erosion. Once again, the morphological effect is similar to that produced by a (small) relative sea-level fall.

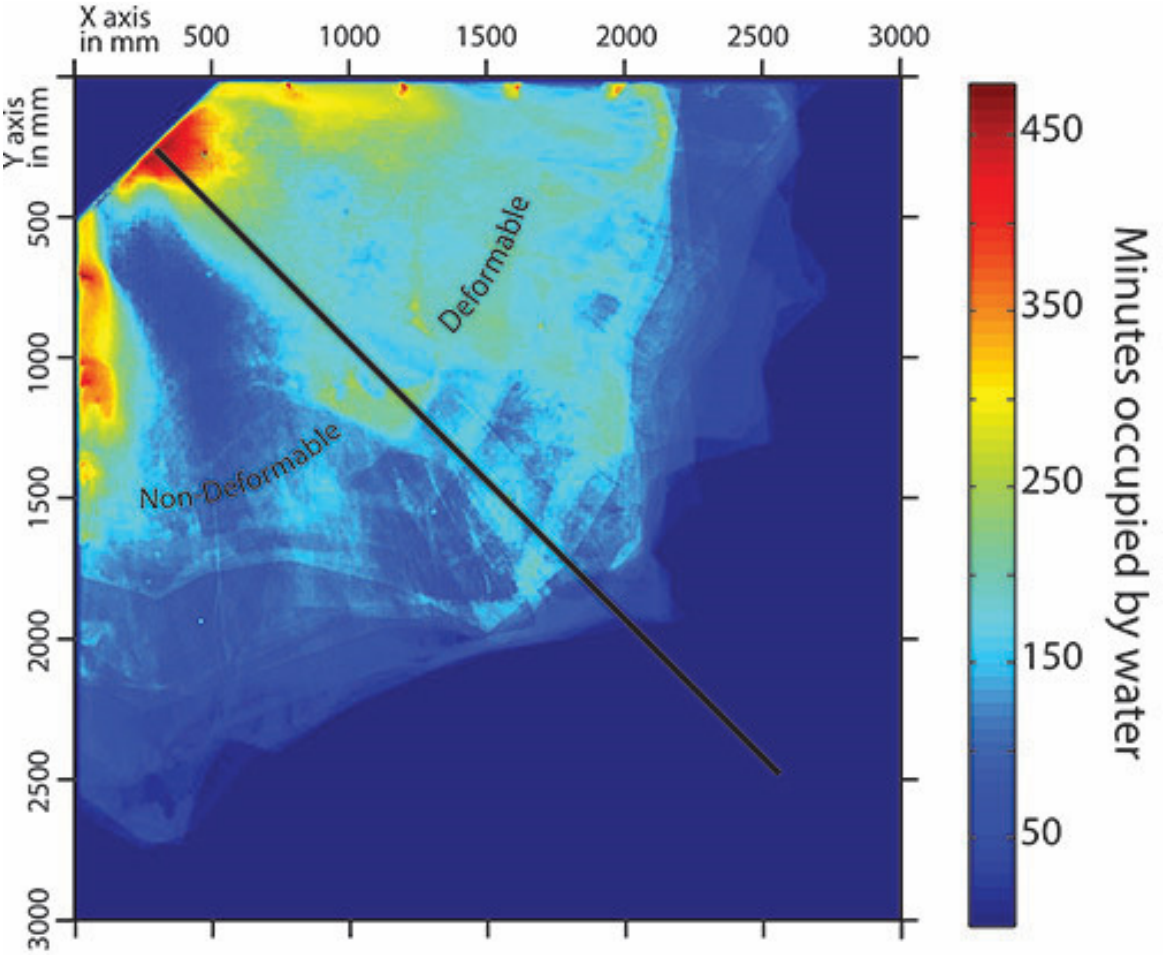

Figure 3-11 Overhead images were analyzed to see the location of water throughout the experiment. The deformable section of the experiment captured 65 percent of the total flow in the experiment.

Chapter 3

DISCUSSION

While the experimental systems shown here are simplified from natural systems, they show clearly the potential for three different forms of offshore dynamics (hyperpycnal turbidity currents, landsliding, and substrate deformation induced by sediment loading) to affect the mass-balance regime of the (topset) fluvial system. Specifically, removing the transport limitation at the clinoform toe (the choke point) switches the fluvial topset system from net deposition to bypass or erosion. The key point is that in each case the change in fluvial system is caused by dynamics occurring well outboard of the shoreline. Stratigraphically, the effect on the fluvial system is similar to that produced by relative sea-level fall, with the proviso that generally speaking the amount of erosion that can be produced by these mechanisms is limited, and the effects would be more localized than those of a eustatic fall. Such changes are commonly ascribed to allogenic forcings, whether sediment supply, eustatic fluctuations, or tectonic changes in accommodation that affect the entire basin (Van Wagoner et al., 1990), or to upstream-sourced autogenic processes such as avulsion. The importance of basin physiography for delta dynamics has been noted in the past (Posamentier and Allen, 1993). However, it has been treated as a static feature rather than a dynamic one as illustrated here.

We return to the "source to sink" concept, which provides a powerful framework to approach mass balance over whole sedimentary systems. However, this paradigm implies one direction of communication, in which climatic and tectonic signals originate in the hinterland and are then propagated downstream. But sediment systems are intrinsically linked, and the propagation of information is bidirectional, i.e. this is a two-way street. The importance of downstream controls has been highlighted via the concept of a sedimentary buttress (Holbrook et al., 2006), but again the main downstream control is generally taken to be relative sea level. Here, we have focused on the influence of transport conditions on the delta foreset and especially the toe as a natural imposed

sediment-flux minimum – a 'choke point' – to illustrate the impact of downstream conditions on upstream behavior. The experimental deltas described here obviously have scales and flow rates much smaller than those observed in natural systems. But we do not see any fundamental aspect of the dynamics by which offshore conditions influence fluvial behavior that is restricted to a particular scale. Indeed, the 'sink to source' framework, like any mechanism arising from mass-balance effects, is scale independent. Thus, we advocate that the 'sink to source' view can be generalized to any transport path in which a local sediment-flux minimum controls upstream deposition.

For example, the effect of scale on one crucial geometric parameter, the foreset slope, can be estimated using the work of Kostic et al. (2002). They showed that overpassing hyperpycnal turbidity currents in a field-scale fluviodeltaic system can reduce delta foreset slopes to 2-3°. Thus the scenario used in our experiments (Case study 1) could unchoke the delta toe on slopes similar to those observed on continental slopes (Pratson and Haxby, 1996). Based on this, a natural setting for clearing the foreset-toe choke point topographically and arresting fluvial deposition is the shelf margin, i.e. where deltas have prograded across the continental shelf and are interacting with the continental slope. Alternatively, the same effect should occur locally wherever clinoforms prograde over the foreset slopes of pre-existing clinoforms (Steckler et al., 1999), or over steep topography created by processes such as mud or salt diapirism (Brown et al., 2004). All of this suggests that episodic clearing of choked clinoform systems, through encounters with pre-existing topography, along with the associated fluvial bypass and offshore sediment transfer, may be relatively common in the geologic record. The stratal impacts of chocked systems may be hard to distinguish between those of low amplitude relative sea level changes or changes in sediment supply, which creates an interesting conundrum and a potentially rich topic for future research.

Chapter 3

CONCLUSIONS

Based on laboratory-scale experiments with self-organized mass flows, deformable substrates, and foreset slope reduction by overpassing hyperpycnal turbidity currents, we find that:

1. Dynamics well outboard of the shoreline can fundamentally change the mass balance in the fluvial (topset) region of a clinoform, leading to a change from net aggradation to bypass or even local erosion, with no changes in sea level or upstream conditions, illustrating a "sink to source" signal propagation.
2. Encounters with offshore sloping topography, combined with hyperpyncnal flow that results in foreset slope reduction can remove the choke condition at the foreset toe and the fluvial system from aggradation to bypass without any changes to base level or upstream conditions.
3. Mass failures in the offshore can temporarily remove the choke condition at the foreset toe, resulting in the formation of upstream migrating knick points in the channel. The formation of these knick points can result in profound changes in the channel morphology and occupancy time, and substantial increases in shoreline rugosity.
4. The presence of a deformable substrate in the deltaic offshore can also temporarily remove the choke condition at the delta toe, leading to changes in rates of delta progradation and channel occupancy.

REFERENCES

Abeyta, A. and **Paola, C.**, 2014, Transport dynamics of mass failures on weakly cohesive clinoform foresets. *Sedimentology*, 62, p. 303-313.

Allen, J.R.L., 1978, Studies in fluviatile sedimentation: an exploratory quantitative model for the architecture of avulsion-controlled alluvial sites. *Sedimentary Geology*, 21, 129-147.

Allen, P., 2008, From landscapes to geological history. *Nature*, 451, p. 274-276.

Blum, M.D., and **Törnqvist, T.E.**, 2000, Fluvial responses to climate and sea-level change: a review and look forward. *Sedimentology*, 47, p. 2–48.

Bown, T.M. and **Kraus, M.J.**, 1987, Integration of channel and floodplain suites, I. developmental sequence and lateral relations of alluvial paleosols. *Journal of Sedimentary Petrology*, 57, p 587-601.

Bridge, J.S., 1997, Thickness of sets of cross strata and planar strata as a function of formative bed-wave geometry and migration, and aggradation rate. *Geology*, 25, p. 971-974.

Bridge, J.S., **Leeder, M.R.**, 1979. A simulation model of alluvial stratigraphy. *Sedimentology*. 26, 617-644.

Brown Jr, L. F., Loucks, R. G., Trevio, R. H., and **Hammes, U.**, 2004, Understanding growth-faulted, intraslope subbasins by applying sequence-stratigraphic principles: Examples from the south Texas Oligocene Frio Formation. *AAPG bulletin*, 88, p. 1501-1522.

Covault, J.A., Romans, B.W., Fildani, A., McGann, M. and **Graham, S.A.**, 2010, Rapid Climatic Signal Propagation from Source to Sink in a Southern California Sediment-Routing System. *Journal of Geology*, 118, p. 247-259.

Carroll, A.R. and **Bohacs, K.M.**, 1999, Stratigraphic classification of ancient lakes: Balancing tectonic and climatic controls. *Geology*, 27, p. 99-102.

Catuneanu, O., 2006, Principles of Sequence Stratigraphy, *Elsevier B.V.*, p. 386.

Chatanantavet, P., Lamb, M. P., and **Nittrouer, J. A.**, 2012, Backwater controls of avulsion location on deltas. *Geophysical Research Letters*, 39, p. 1-6.

Duller, R.A., Whittaker, A.C., Fedele, J.J., Whitchurch, A.L., Springett, J., Smithells, R., Fordyce, S., and **Allen, P.A.**, 2010, From grain size to tectonics. *Journal of Geophysical Research: Earth Surface*, 115, F03022.

Fisk, N.H., 1944, Geological Investigation of the Alluvial Valley of the Lower Mississippi River. *Mississippi River Commission, Vicksburg, MS.*

Foreman, B.Z., 2014, Climate-driven generation of a fluvial sheet sand body at the Paleocene-Eocene boundary in north-west Wyoming (U.S.A.). *Basin Research*, 26, p. 225-241.

Foreman, B.Z., Heller, P.L., and **Clementz, M.T.**, 2012. Fluvial response to abrupt global warming at the Palaeocene/Eocene boundary. *Nature*, 491, p. 92-95.

Friedrichs, C.T., and **Scully, M.E.**, 2007, Modeling deposition by wave-supported gravity flows on the Po River prodelta: From seasonal floods to prograding clinoforms. *Continental Shelf Research*, 27, 322-337.

Hajek, E.A., Heller, P.L., and **Sheets, B.A.**, 2010, Significance of channel-belt clustering in alluvial basins. *Geology*, 38, p. 535-538.

Hajek, E.A., Heller, P.L., and **Shur, E.L.**, 2012, Field test of autogenic control on alluvial stratigraphy (Ferris Formation, Upper Cretaceous-Paleogene, Wyoming). *GSA Bulletin*, 124, p. 1898-1912.

Helland-Hansen, and **W., Martinsen, O.J**, 1996, Shoreline trajectories and sequences: Description of variable depositional-dip scenarios. *Journal of Sedimentary Research*, 66, p. 670-688.

Hudec, M. R., and **Jackson, M.**, 2007, Terra infirma: Understanding salt tectonics. *Earth-Science Reviews*, 82, p.1-28.

Holbrook, J., Scott, R. W., and **Oboh-Ikuenobe, F. E.,** 2006, Base-level buffers and buttresses: a model for upstream versus downstream control on fluvial geometry and architecture within sequences. *Journal of Sedimentary Research*, 76, p. 162-174.

Hoyal, D., and **Sheets, B.**, 2009, Morphodynamic evolution of experimental cohesive deltas. *Journal of Geophysical Research: Earth Surface*, 14, F2, p. F02009.

Kineke, G., Sternberg, R.W., Trowbridge, J.H., and **Geyer, R.W.**, 1996, Fluid mud processes on the Amazon continental shelf. *Continental Shelf Research*, v. 16, p. 676-696.

Kostic, S., Parker, G., and **Marr, J.G.**, 2002, Role of turbidity currents in setting the foreset slope clinoforms prograding into standing fresh water. *Journal of Sedimentary Research*, 72, p. 353–362.

Kraus, M.J., 1997, Lower Eocene alluvial paleosols: Pedogenic development, stratigraphic relationships, and paleosols/landscape associations. *Palaeogeography, Palaeoclimatology, Palaeoecology,* 129, p. 387-406.

Lamb, M. P., Nittrouer, J. A., Mohrig, D., and **Shaw, J.**, 2012, Backwater and river plume controls on scour upstream of river mouths: Implications for fluvio-deltaic morphodynamics. *Journal of Geophysical Research: Earth Surface*, 117, F1, p. 2003–2012.

Leeder, M.R., 1978, A quantitative stratigraphic model for alluvium, with special reference to channel deposit density and interconnectedness in: Miall, A.D. (Ed.), *Memoirs of the Canadian Society of Petroleum Geology,* 5, pp. 587-596.

Madof, A. S., Christie-Blick, N., and **Anders, M. H.**, 2009, Stratigraphic controls on a salt-withdrawal intraslope minibasin, north-central Green Canyon, Gulf of Mexico: Implications for misinterpreting sea level change. *AAPG bulletin*, 93, p. 535-561.

Paola, C., 2000, Quantitative models of sedimentary basin filling. *Sedimentology*, 47, p. 121–178.

Paola, C. and **Borgman, L.**, 1991, Reconstructing random topography from preserved stratification. *Sedimentology*, 38, 553-565.

Penck, A., and **Bruckner, E.**, 1909, Die Alpen im Eiszeitalter, Tauchnitz, Leipzig.

Piliouras, A., Kim, W., Kocurek, G. A., Mohrig, D., and **Kopp, J.**, 2014, Sand on salt: Controls on dune subsidence and determining salt substrate thickness. *Lithosphere*, 6, p. 195-199.

Posamentier, H.W., and **Allen, G.P.**, 1993, Variability of the sequence stratigraphic model: effects of local basin factors. *Sedimentary Geology,* 86, p. 91-109.

Porebski, S.J., and **Steel, R.J.**, 2003, Shelf-margin deltas: their stratigraphic significance and relation to deepwater sands. *Earth-Science Reviews*, 62, p. 283-326.

Schellart, W.P., 2011, Rheology and density of glucose syrup and honey: Determining their suitability for usage in analogue and fluid dynamic models of geological processes. *Journal of Structural Geology,* 33, p. 1079-1088.

Schumm, S.A., 1993, River response to base level change: Implications for sequence stratigraphy. *Journal of Geology*, 101, p. 279-294.

Sloss, L.L., 1962, Stratigraphic models in exploration. *Journal of Sedimentary Petrology*, 32, p. 415-422.

Straub, K.M., Paola, C., Mohrig, D., Wolinsky, M.A., and **George, T.**, 2009, Compensational stacking of channelized sedimentary deposits. *Journal of Sedimentary Research*, 79, p. 673-688.

Straub, K.M. and **Pyles, D.R.**, 2012, Quantifying the hierarchical organization of compensation in submarine fans using surface statistics. *Journal of Sedimentary Research*, 82, p. 889-898.

Webster, K. L., Ogston, A. S., and **Nittrouer, C. A.**, 2013, Delivery, reworking and export of fine-grained sediment across the sandy Skagit River tidal flats, *Continental Shelf Research*, 60, p. S58-S70.

Weijermars, R., Jackson, M.P.A., and **Vendeville, B.**, 1993, Rheological and tectonic modeling of salt provinces. **Tectonophysics**, 217, p. 143-174.

Whittaker, A.C., Attal, M., and **Allen, P.A.**, 2010, Characterising the origin, nature and fate of sediment exported from catchments perturbed by active tectonics. *Basin Research*, 22, p. 809-828.

Van Wagoner, J.C., Mitchum, R.M., Campion, K.M., and **Rahmanian, V.D.,** 1990, Siliciclastic sequence stratigraphy in well logs, cores, and outcrops. Tulsa, Oklahoma. *American Association of Petroleum Geologists Methods in Exploration Series*, 7, p. 55.

Voller, V. R., Ganti, V., Paola, C., and **Foufoula-Georgiou, E.**, 2012, Does the flow of information in a landscape have direction? *Geophysical Research Letters*, 39, L01403.

4

OVERALL CONCLUSION

The most current approach in understanding coastal and deltaic systems is to ascribe the many shapes and features observed in the deposits to external forces (relative fluvial, tidal, and wave effects) acting on the system (Galloway, 1975). In many ways, this dissertation is focused on exploring different avenues to explain phenomena in coastal depositional systems, by looking at the role of grain scale and addressing the question of how small scale interactions lead to large scale, measurable behavior in coastal and deltaic depositional systems. In the previous chapters, we have developed new methods to introduce cohesive sediment into physical laboratory experiments, which creates important geomorphic thresholds that regulate the transport and behavior of grains. Throughout these chapters, we have established metrics to quantify how the presence of cohesive sediment changes these systems in terms of failure events, planform morphology and changes in the sediment mass balance.

Through our experiments, we have found that:

1. The addition of cohesive sediment alters the behavior of the foreset away from regular small avalanches to a range of mass failures including intermittently large events.
2. There is no correlation between sediment and water discharge and the size or frequency of avalanche events but rather increases in discharge are accounted for by increases of slow creeping of the sediment.

3. Without any way of constraining the rates of shearing, it would be difficult to distinguish deposits formed as the result of slow creep and those that are rapidly deposited.

4. Cohesive sediment alters morphological properties on deltaic systems, in particular changing channel morphology, channel occupancy time, avulsion style, bar deposition and shoreline shape.

5. Offshore events well outboard of the shoreline fundamentally change the mass balance of coastal depositional systems, leading to changes from deposition to bypass or local erosion, without any changes in sea level or upstream conditions.

Although the experiments presented here are much simpler than natural systems, our results suggest that grain-scale changes as the result of cohesive sediment lead to large-scale, measurable changes in coastal depositional systems, giving merit to Victor Hugo's observation of the large scale world being created at the granular level (Hugo, 1862). While there has not been a comprehensive study looking at the role of cohesion in setting geomorphic features of deltas in the field, the experiments described here highlight some of the trends we expect to find in different field cases. For example, metrics such as increases in shoreline complexity as measured by the area-deficit ratio represent an easily measureable parameter that can be applied to modern deltas, and even to ancient examples where they are well imaged seismically (Posamentier et al., 1992; Deptuck et al., 2012).

FUTURE DIRECTIONS

We believe physical experiments that include cohesive sediment represent an important geomorphic threshold, which may be crucial to understanding deltaic morphology. The experiments presented here demonstrate the importance and impact of cohesive sediment, however they do not cover the full range of possibilities. It would be an interesting avenue of investigation to expand upon these experiments to cover the full range of conditions, similar to the numerical modeling work done by Edmonds and

Slingerland (2009). In addition to expanding the suite of experiments, it would be interesting to compare the numerical and physical modeling results to field cases.

Secondly, it would be worth investigating further how flocculated clay sediment alters the depositional behavior and morphology of coastal deltaic systems. There is an increasing amount of research that shows clays are commonly transported in the form of aggregates (flocs), which changes the physical properties of the grains being transported such as density, grain size, and settling velocity (Schieber, 2007). Most models of clay transport and deposition do not incorporate this idea (e.g., Van Rijn, 1984), despite there being clear evidence that flocculation changes the mode of transport (Schieber et al., 2007). Preliminary experiments presented here do demonstrate that flocculation affects morphological properties, such as reduced shoreline complexity and channel migration rates. It is uncertain to what extent the form of the clay sediment (aggregated vs non-aggregated) influences and alters morphological behavior. Further work on constraining the impacts of flocculation on patterns of transport and deposition in coastal deltaic settings would prove useful for understanding the morphodynamics of these systems.

The experiments presented here demonstrate that there are measurable, morphodynamic changes in sedimentary systems when cohesive sediment is added. However, these experiments are preliminary in understanding the appropriate modifications that are necessary to our current framework of depositional systems. Many of the world's coastal deltaic systems are feeling the consequences of what were once feats of human engineering, where these bountiful landscapes are being starved of sediment and drowning in encroaching seas (Syvitski et al., 2009). Sediment is the lifeblood of these systems and with fine grained sediments (silts and clays) making upwards of 80 percent of the world's sediment budgets, it is becoming increasingly important to understand the patterns of fine sediment transport and deposition (Milliman and Syvitski, 1992).

REFERENCES

Deptuck, M.E., Mohrig, D., Van Hoorn, B., and **Wynn, R.B.**, 2012, Application of the principles of seismic geomorphology to the continental slope and base of slope systems: Case studies from sea floor and near shore analogs. *Society of Sedimentary geology*, p. 145-161.

Edmonds, D. and **Slingerland, R.**, 2009, Significant effect of sediment cohesion on delta morphology. *Nature Geoscience*, 3, p. 105-109.

Galloway, W., 1975, Process Framework for Describing the Morphology and Stratigraphic Evolution of Deltaic Depositional Systems. *Deltas Models for Exploration*, p. 87-98.

Hugo, V., 1862, *Les Miserables*

Milliman, J.D. and **Syvitski, J. P. M.**, 1992, Geomorphic/tectonic control of sediment discharge to the oceans: the importance of small mountainous rivers. *Journal of Geology*, 100, p. 525-544.

Posamentier, H.W., Allen, G.P., and **James, D P.**, 1992, High resolution sequence stratigraphy- the east Coulee Delta, Alberta. *Journal of Sedimentary Research*, 62, no. 2.

Schieber, J., Southard, J., and **Theison, K.**, 2007, Accretion of Mudstone Beds from Migrating Floccule Ripples. *Science*, 318, p. 1760-1763.

Syvitski, J. P., Kettner, A. J., Overeem, I., Hutton, E. W., Hannon, M. T., Brakenridge, G. R., Day, J., Vörösmarty, C., Saito, Y., Giosan, L. and **Nicholls, R. J.**, 2009, Sinking deltas due to human activities. *Nature Geoscience*, 2, p. 681-686.

Van Rijn, L., 1984, Sediment Transport, part II: Suspended Sediment Load. *Journal of Hydraulic Engineering*, Vol. 110, no. 11, p. 1613-1641.

COMPREHENSIVE REFERENCES

Abeyta, A. and **Paola, C.**, 2014, Transport dynamics of mass failures on weakly cohesive clinoform foresets. *Sedimentology*, 62, p. 303-313.

Allen, J.R.L., 1978, Studies in fluviatile sedimentation: an exploratory quantitative model for the architecture of avulsion-controlled alluvial sites. *Sedimentary Geology*, 21, 129-147.

Allen, P., 2008, From landscapes to geological history. *Nature*, 451, p. 274-276.

Bain, R., 2014, A Comparison of the Planforms of Meandering Tidal and Fluvial Channels on the Ganges-Brahmaputra-Jamuna Delta, Bangladesh. (Master's Thesis), *University of Minnesota.*

Bea, R. (1971) How sea floor slides affect offshore structures. *Oil & Gas journal*, **69**, 88-91.

Blum, M.D., and **Törnqvist, T.E.**, 2000, Fluvial responses to climate and sea-level change: a review and look forward. *Sedimentology*, 47, p. 2–48.

Bown, T.M. and **Kraus, M.J.**, 1987, Integration of channel and floodplain suites, I. developmental sequence and lateral relations of alluvial paleosols. *Journal of Sedimentary Petrology*, 57, p 587-601.

Bridge, J.S., 1997, Thickness of sets of cross strata and planar strata as a function of formative bed-wave geometry and migration, and aggradation rate. *Geology*, 25, p. 971-974.

Bridge, J.S., **Leeder, M.R.**, 1979. A simulation model of alluvial stratigraphy. *Sedimentology*. 26, 617-644.

Brown Jr, L. F., Loucks, R. G., Trevio, R. H., and **Hammes, U.**, 2004, Understanding growth-faulted, intraslope subbasins by applying sequence-stratigraphic principles:

Examples from the south Texas Oligocene Frio Formation. *AAPG bulletin*, 88, p. 1501-1522.

Bruschi, R., Bughi, S., Spinazzé, M., Torselletti, E., and **Vitali, L.** (2006) Impact of debris flows and turbidity currents on seafloor structures. *Norwegian Journal of Geology*, **86**, 317-336.

Carson, R. (1951) The long snowfall. Oxford Publishing: pp. 75-83.

Covault, J.A., Romans, B.W., Fildani, A., McGann, M. and **Graham, S.A.**, 2010, Rapid Climatic Signal Propagation from Source to Sink in a Southern California Sediment-Routing System. *Journal of Geology*, 118, p. 247-259.

Carroll, A.R. and **Bohacs, K.M.**, 1999, Stratigraphic classification of ancient lakes: Balancing tectonic and climatic controls. *Geology*, 27, p. 99-102.

Catuneanu, O., 2006, Principles of Sequence Stratigraphy, *Elsevier B.V.*, p. 386.

Chatanantavet, P., Lamb, M. P., and **Nittrouer, J. A.**, 2012, Backwater controls of avulsion location on deltas. *Geophysical Research Letters*, 39, p. 1-6.

Deptuck, M.E., Mohrig, D., Van Hoorn, B., and **Wynn, R.B.**, 2012, Application of the principles of seismic geomorphology to the continental slope and base of slope systems: Case studies from sea floor and near shore analogs. *Society of Sedimentary geology*, p. 145-161.

Duller, R.A., Whittaker, A.C., Fedele, J.J., Whitchurch, A.L., Springett, J., Smithells, R., Fordyce, S., and **Allen, P.A.**, 2010, From grain size to tectonics. *Journal of Geophysical Research: Earth Surface*, 115, F03022.

Edmonds, D. and **Slingerland, R.**, 2009, Significant effect of sediment cohesion on delta morphology. *Nature Geoscience*. 3, p. 105-109.

Edmonds, D. A., Paola, C., Hoyal, D. C., and **Sheets, B. A.**, 2011, Quantitative metrics that describe river deltas and their channel networks. *Journal of Geophysical Research: Earth Surface,* 116, 2003-2012.

Fagherazzi, S., Gabet, E. J., and **Furbish, D. J.**, 2004, The effect of bidirectional flow on tidal channel planforms. *Earth Surface Processes and Landforms*, 29, p. 295-309.

Fisk, N.H., 1944, Geological Investigation of the Alluvial Valley of the Lower Mississippi River. *Mississippi River Commission, Vicksburg, MS.*

Foreman, B.Z., 2014, Climate-driven generation of a fluvial sheet sand body at the Paleocene-Eocene boundary in north-west Wyoming (U.S.A.). *Basin Research*, 26, p. 225-241.

Foreman, B.Z., Heller, P.L., and **Clementz, M.T.**, 2012. Fluvial response to abrupt global warming at the Palaeocene/Eocene boundary. *Nature*, 491, p. 92-95.

Friedrichs, C.T., and **Scully, M.E.**, 2007, Modeling deposition by wave-supported gravity flows on the Po River prodelta: From seasonal floods to prograding clinoforms. *Continental Shelf Research*, 27, 322-337.

Galloway, W., 1975, Process Framework for Describing the Morphology and Stratigraphic Evolution of Deltaic Depositional Systems. *Deltas Models for Exploration*, p. 87-98.

Gastaldo, R. A., Allent, G., and **Huci, A. Y.**, 2009, The tidal character of fluvial sediments of the modern Mahakam River delta, Kalimantan, Indonesia. *Tidal Signatures in Modern and Ancient Sediments (Special Publication 24 of the IAS)*, 28, 171.

Gerber, T., Pratson, L., Wolinsky, M., Steel, R., Mohr, J., Swenson, J. and **Paola, C**. (2008) Clinoform progradation by turbidity currents: Modeling and experiments. *Journal of Sedimentary Research*, **78**, 220-238.

Hajek, E.A., Heller, P.L., and **Sheets, B.A.**, 2010, Significance of channel-belt clustering in alluvial basins. *Geology*, 38, p. 535-538.

Hajek, E.A., Heller, P.L., and **Shur, E.L.**, 2012, Field test of autogenic control on alluvial stratigraphy (Ferris Formation, Upper Cretaceous-Paleogene, Wyoming). *GSA Bulletin*, 124, p. 1898-1912.

Helland-Hansen, and **W., Martinsen, O.J**, 1996, Shoreline trajectories and sequences: Description of variable depositional-dip scenarios. *Journal of Sedimentary Research*, 66, p. 670-688.

Heezen, B., and **Ewing, M.** (1952) Turbidity currents and submarine slumps, and the 1929 Grand Banks Earthquake. *American Journal of Science*, **250**, 849-873.

Hudec, M. R., and **Jackson, M.**, 2007, Terra infirma: Understanding salt tectonics. *Earth-Science Reviews*, 82, p.1-28.

Hugo, V., 1862, *Les Miserables.*

Holbrook, J., Scott, R. W., and **Oboh-Ikuenobe, F. E.,** 2006, Base-level buffers and buttresses: a model for upstream versus downstream control on fluvial geometry and architecture within sequences. *Journal of Sedimentary Research*, 76, p. 162-174.

Hoyal, D., and **Sheets, B.**, 2009, Morphodynamic evolution of experimental cohesive deltas. *Journal of Geophysical Research: Earth Surface*, 14, F2, p. F02009.

Kenyon, P. and **Turcotte, D.** (1985) Morphology of a delta prograding by bulk sediment transport. *Geological Society of America Bulletin*, **96**, 1457-1465.

Keshavarzi, A. and **Habbi, L.**, 2005, Optimizing water intake angle by flow separation analysis. *Irrigation Drainage*, 54, p. 543-552.

Kineke, G., Sternberg, R.W., Trowbridge, J.H., and **Geyer, R.W.**, 1996, Fluid mud processes on the Amazon continental shelf. *Continental Shelf Research*, v. 16, p. 676-696.

Komatsu, T., Inagaki, S., Nakagawa, N., and **Nasuno, S.** (2000) Creep motion in a granular pile exhibiting steady surface flow. *Physical Review Letters*, **86**, 1757-1760.

Kostic, S., Parker, G., and **Marr, J.G.**, 2002, Role of turbidity currents in setting the foreset slope clinoforms prograding into standing fresh water. *Journal of Sedimentary Research*, 72, p. 353–362.

Kraus, M.J., 1997, Lower Eocene alluvial paleosols: Pedogenic development, stratigraphic relationships, and paleosols/landscape associations. *Palaeogeography, Palaeoclimatology, Palaeoecology,* 129, p. 387-406.

Lamb, M. P., Nittrouer, J. A., Mohrig, D., and **Shaw, J.**, 2012, Backwater and river plume controls on scour upstream of river mouths: Implications for fluvio-deltaic morphodynamics. *Journal of Geophysical Research: Earth Surface*, 117, F1, p. 2003–2012.

Larsen, L., Harvey, J.W, Noe, G.B., and **Crimaldi, J.P**., 2009, Predicting organic floc transport dynamics in shallow aquatic ecosystems: Insights from the field, the laboratory, and numerical modeling. *Water resources Research*, 42, W01411.

Leeder, M.R., 1978, A quantitative stratigraphic model for alluvium, with special reference to channel deposit density and interconnectedness in: Miall, A.D. (Ed.), *Memoirs of the Canadian Society of Petroleum Geology,* 5, pp. 587-596.

Levin, D. R., 1995, Occupation of a relict distributary system by a new tidal inlet, Quatre Bayou Pass, Louisiana. *Tidal Signatures in Modern and Ancient Sediments. Special Publication 24 of the IAS*, 9, 71.

Martin, J., Sheets, B., Paola, C., and **Hoyal, D.**, 2009-A, Influence of steady base-level rise on channel mobility, shoreline migration, and scaling properties of a cohesive experimental delta. *Journal of Geophysical Research*, 144, F3, F03017.

Martin, J., Paola, C., Abreu, V, Neal, J., and **Sheets, B.**, 2009-B, Sequence stratigraphy of experimental strata under known conditions of differential subsidence and variable base level. *AAPG Bulletin*, 93, p. 503-533.

Madof, A. S., Christie-Blick, N., and **Anders, M. H.**, 2009, Stratigraphic controls on a salt-withdrawal intraslope minibasin, north-central Green Canyon, Gulf of Mexico: Implications for misinterpreting sea level change. *AAPG bulletin*, 93, p. 535-561.

Marr J., Harff, P., Shanmugam, G., and **Parker, G.** (2001) Experiments on subaqueous sandy gravity flows: The role of clay and water content on flow dynamics and depositional structures. *Geological Society of America Bulletin*, 1377-1386.

Masson, D.G., Harbitz, C.B., Wynn, R.B., Pedersen, G., and **Løvholt, F.** (2006) Submarine landslides: processes, triggers and hazard prediction. *Philosophical Transactions of the Royal Society A*, **364**, 2009-2039.

Milliman, J.D. and **Syvitski, J. P. M.**, 1992, Geomorphic/tectonic control of sediment discharge to the oceans: the importance of small mountainous rivers. *Journal of Geology*, 100, p. 525-544.

Miyamoto, H., Baker, V. R., and **Lorenz, R. D.**, 2005, Entropy and the Shaping of the Landscape by Water, *Springer Berlin Heidelberg*, Ch. 11, p. 135-146.

Mohrig D., and **Marr, J.** (2003) Constraining the efficiency of turbidity current generation from submarine debris flows and slides using laboratory experiments. *Marine and Petroleum Geology*, **20**, 884-889.

Nittrouer, J. A., Best, J. L., Brantley, C., Cash, R. W., Czapiga, M., Kumar, P., and **Parker, G.**, (2012), Mitigating land loss in coastal Louisiana by controlled diversion of Mississippi River sand, *Nature Geoscience*, 5, p. 534-537.

Orton, G. and **Reading, H.**, 1993, Variability of deltaic processes in terms of sediment supply, with particular emphasis on grain size. *Sedimentology*, 40, p. 475-512.

Paola, C., 2000, Quantitative models of sedimentary basin filling. *Sedimentology*, 47, p. 121–178.

Paola, C. and **Borgman, L.**, 1991, Reconstructing random topography from preserved stratification. *Sedimentology*, 38, 553-565.

Paola, C., Mullin, J., Ellis, C., Mohrig, D., Swenson, J.B., Parker, G., Hickson, T., Heller, P., Pratson, L., Syvitski, J., Sheets, B., and **Strong, N.**, 2001, Experimental stratigraphy. *GSA Today*, 11, p. 4-9.

Parker, H., 1996, River meandering as self-organization process. *Science*, 271, pp. 1710.

Parker, G., Garcia, M., Fukushima, Y., and **Yu, W.** (1987) Experiments on turbidity currents over an erodible bed. *Journal of Hydraulic Research,* **25**, 123-147.

Parsons, J., Friedrichs, C., Traykovski, P., Syvitski, J., Parker, G., Puig, P., Buttles, J., and **Garcia, M.** (2007) The mechanics of marine sediment gravity flows. *International Association of Sedimentologists Special Publication,* **37**, 275-337.

Passalacqua, P., Lanzoni, S., Paola, C., and **Rinaldo, A.**, 2013, Geomorphic signatures of deltaic processes and vegetation: The Ganges-Brahmaputra-Jamuna case study. *Journal of Geophysical Research: Earth Surface*, 118, p. 1838-1849.

Penck, A., and **Bruckner, E.**, 1909, Die Alpen im Eiszeitalter, Tauchnitz, Leipzig.

Piliouras, A., Kim, W., Kocurek, G. A., Mohrig, D., and **Kopp, J.**, 2014, Sand on salt: Controls on dune subsidence and determining salt substrate thickness. *Lithosphere*, 6, p. 195-199.

Piper, D., and **Normark, W.** (2009) Processes that initiate turbidity currents and their influence on turbidites: A marine geology perspective. *Journal of Sedimentary Research*, **79**, 347-362.

Pirmez, C., 1998, Clinoform development by advection-diffusion of suspended sediment: Modeling and comparison to natural systems. *Journal of Geophysical Research*, 103, p. 24,141–24,175.

Posamentier, H.W., Allen, G.P., and **James, D P.**, 1992, High resolution sequence stratigraphy- the east Coulee Delta, Alberta. *Journal of Sedimentary Research*, 62, no. 2.

Posamentier, H.W., and **Allen, G.P.**, 1993, Variability of the sequence stratigraphic model: effects of local basin factors. *Sedimentary Geology,* 86, p. 91-109.

Porebski, S.J., and **Steel, R.J.**, 2003, Shelf-margin deltas: their stratigraphic significance and relation to deepwater sands. *Earth-Science Reviews*, 62, p. 283-326.

Schellart, W.P., 2011, Rheology and density of glucose syrup and honey: Determining their suitability for usage in analogue and fluid dynamic models of geological processes. *Journal of Structural Geology,* 33, p. 1079-1088.

Schieber, J. and **Zimmerle, W.**, 1998, The history and promise of shale research. *Shales and mudstones, 1, Basin studies of sedimentology and paleontology*, p. 1-10

Schieber, J., Southard, J., and **Theison, K.**, 2007, Accretion of Mudstone Beds from Migrating Floccule Ripples. *Science*, 318, p. 1760-1763.

Schieber, J. and **Southard, J.,** 2009-a, Bedload transport of mud by floccule ripples – Direct observations of ripple migration processes and their implications. *Geology*, 37, p. 483-486.

Schieber, J. and **Yawar, Z.,** (2009-b) A New Twist on Mud Deposition – Mud Ripples in Experiment and Rock Record. The Sedimentary Record: Vol. 7, no. 2, pp. 4-8.

Schumm, S.A., 1993, River response to base level change: Implications for sequence stratigraphy. *Journal of Geology*, 101, p. 279-294.

Sloss, L.L., 1962, Stratigraphic models in exploration. *Journal of Sedimentary Petrology*, 32, p. 415-422.

Smart, J. S., and **Moruzzi, V. L.**, 1971, Quantitative properties of delta channel networks. IBM Thomas J Watson Research Center, Yorkston Heights, NY, No. Tr-3.

Straub, K.M., Paola, C., Mohrig, D., Wolinsky, M.A., and **George, T.**, 2009, Compensational stacking of channelized sedimentary deposits. *Journal of Sedimentary Research*, 79, p. 673-688.

Straub, K.M. and **Pyles, D.R.**, 2012, Quantifying the hierarchical organization of compensation in submarine fans using surface statistics. *Journal of Sedimentary Research*, 82, p. 889-898.

Syvitski, J. P., Kettner, A. J., Overeem, I., Hutton, E. W., Hannon, M. T., Brakenridge, G. R., Day, J., Vörösmarty, C., Saito, Y., Giosan, L. and **Nicholls, R. J.**, 2009, Sinking deltas due to human activities. *Nature Geoscience*, 2, p. 681-686.

Van Rijn, L., 1984, Sediment Transport, part II: Suspended Sediment Load. *Journal of Hydraulic Engineering*, Vol. 110, no. 11, p. 1613-1641.

Van Wagoner, J.C., Mitchum, R.M., Campion, K.M., and **Rahmanian, V.D.,** 1990, Siliciclastic sequence stratigraphy in well logs, cores, and outcrops. Tulsa, Oklahoma. *American Association of Petroleum Geologists Methods in Exploration Series*, 7, p. 55.

Voller, V. R., Ganti, V., Paola, C., and **Foufoula-Georgiou, E.**, 2012, Does the flow of information in a landscape have direction? *Geophysical Research Letters*, 39, L01403.

Webster, K. L., Ogston, A. S., and **Nittrouer, C. A.**, 2013, Delivery, reworking and export of fine-grained sediment across the sandy Skagit River tidal flats, *Continental Shelf Research*, 60, p. S58-S70.

Weijermars, R., Jackson, M.P.A., and **Vendeville, B.**, 1993, Rheological and tectonic modeling of salt provinces. **Tectonophysics**, 217, p. 143-174.

Weiner, L., 1991, Walker Art Center.

Whittaker, A.C., Attal, M., and **Allen, P.A.**, 2010, Characterising the origin, nature and fate of sediment exported from catchments perturbed by active tectonics. *Basin Research*, 22, p. 809-828.

Wright, L., and **Friedrichs, C.** (2006) Gravity-driven sediment transport on continental shelves: A status report. *Continental Shelf Research*, **26**, 2092-2107.